



Fire use and waste management in an Iberian Iron Age village: Geoarchaeological insights into midden formation processes

Laura Tomé^{a,b,*}, Eneko Iriarte^c, Antonio Blanco-González^d, Enrique Fernández-Palacios^{a,b},
María Martín-Seijo^e, Ángel Carrancho^f, Antonio V. Herrera-Herrera^{a,g}, Carolina Mallol^{a,b,h}

^a Archaeological Micromorphology and Biomarkers Laboratory (AMBI Lab), Instituto Universitario de Bio-Orgánica “Antonio González”, Universidad de La Laguna, 38206 Tenerife, Spain

^b Área de Prehistoria, Departamento de Geografía e Historia, Facultad de Humanidades, Universidad de La Laguna, 38206 Tenerife, Spain

^c Laboratorio IsoTOPIK-Laboratorio de Evolución Humana, Departamento de Historia, Geografía y Comunicación, Facultad de Humanidades y Comunicación, Universidad de Burgos, 09001 Burgos, Spain

^d Research Group PREHUSAL, Departamento de Prehistoria, Historia Antigua y Arqueología, Facultad de Geografía e Historia, Universidad de Salamanca, 37002 Salamanca, Spain

^e Instituto de Ciencias del Patrimonio (INCIPIT), Consejo Superior de Investigaciones Científicas (CSIC), Edificio Fontan, Bloque 4, Monte Gaias, s/n. 15707 Santiago de Compostela, Spain

^f Área de Prehistoria, Departamento de Historia, Geografía y Comunicación, Universidad de Burgos, 09001, Burgos, Spain

^g Departamento de Química, Unidad Departamental de Química Analítica, Facultad de Ciencias, Universidad de La Laguna, 38206 Tenerife, Spain

^h Interdisciplinary Center for Archaeology and the Evolution of Human Behaviour (ICArEHB), Universidade do Algarve, Campus de Gambelas, Edifício 1, 8005-139 Faro, Portugal

ARTICLE INFO

Keywords:

Geoarchaeology
Micromorphology
Lipid biomarkers
Iron Age
Combustion features
Midden

ABSTRACT

Middens, commonly found in archaeological sites across different chronologies, serve as rich sedimentary archives of daily life by capturing the refuse and discarded artifacts of past human groups. This study focuses on the midden deposits of the Early Iron Age settlement site of Cerro de San Vicente (Central Iberia). We applied a high-resolution, microcontextual geoarchaeological approach, integrating soil micromorphology—including phytolith and charcoal analyses on thin sections—, sedimentary lipid biomarker analysis, X-Ray fluorescence (XRF), X-Ray diffraction (XRD) and magnetic properties analysis to investigate the formation processes and past functionality of the site's midden deposits. Our findings reveal that the targeted sequences are primarily composed of wood ash and charred plant refuse, as well as trampled and disintegrated earth-based construction materials. These deposits are interpreted as the result of multiple hearth rake-out events, maintenance and construction activities, and possible spatially-related communal storage practices within the village. Stratigraphic connections between deposits from inside and outside the dwellings are proposed, linking the middens to an intermediate phase (ca. 600 BCE) of the village's history. These results offer relevant insights into the spatial and temporal dynamics of refuse disposal, maintenance practices and space use at Cerro de San Vicente, highlighting the value of microcontextual geoarchaeological methods in unveiling domestic practices. This study contributes to enhancing our understanding of Early Iron Age socio-cultural and daily life practices in Central Iberia.

1. Introduction

1.1. Midden deposits: Sedimentary archives of daily life

Middens are common sedimentary deposits found in archaeological sites across various chronologies and geographic locations. These deposits are typically identified through macroscopic field observations

and are characterized as accumulations of discarded archaeological items and artifacts, resulting from anthropogenic or cultural formation processes (Brönnimann et al., 2020; Shillito, 2015) as opposed to natural, biogenic, or geogenic processes. According to Schiffer (1972), archaeological objects are typically discarded when their use-life has concluded, transforming into *refuse*—items that have lost their cultural functionality within a social group. Refuse accumulations—that is,

* Corresponding author at: Archaeological Micromorphology and Biomarkers Laboratory (AMBI Lab), Instituto Universitario de Bio-Orgánica “Antonio González”, Universidad de La Laguna, 38206 Tenerife, Spain.

E-mail address: lhernant@ull.edu.es (L. Tomé).

<https://doi.org/10.1016/j.jasrep.2024.104773>

Received 5 July 2024; Received in revised form 11 September 2024; Accepted 12 September 2024

Available online 21 September 2024

2352-409X/© 2024 The Author(s). Published by Elsevier Ltd. This is an open access article under the CC BY license (<http://creativecommons.org/licenses/by/4.0/>).

midden deposits— may include actively or passively discarded items, some of which might remain usable (Needham and Spence, 1997; Schiffer, 1972).

Artifacts unearthed in middens are intricately linked to daily life and cultural practices, making them invaluable archaeological remains for comprehending human behavior (Beck and Hill, 2004; Hayden and Cannon, 1983; Needham and Spence, 1997; Schiffer, 1976; Shillito, 2015). These contexts are pivotal for assessing past cultural and socio-economic practices and paleoenvironments due to their propensity for preserving a wealth of artifacts and biological remains, surpassing the richness found in other settings, such as buildings (Shillito and Matthews, 2013). While dump deposits have been recorded since Paleolithic and Mesolithic times (Aldeias et al., 2012; Aldeias and Bicho, 2016; Duarte et al., 2019; Goldberg et al., 2003; Marcuzzan et al., 2022; Meignen et al., 2007; Schiegl et al., 2003; Starkovich et al., 2020), their occurrence significantly increases with the onset of the Holocene, due to the proliferation and intensification of sedentism and urban life, from the Neolithic period onward (Brönnimann et al., 2020; Butler et al., 2020; Debels et al., 2024; Gutiérrez-Rodríguez et al., 2022; Oikonomou, 2023; Shahack-Gross et al., 2023; Shillito et al., 2011b, 2008; Shillito and Mackay, 2020; Shillito and Matthews, 2013; Stahlschmidt et al., 2017).

Despite variations in chronology and their heterogeneous content—ranging from discarded shells and/or animal bone (Aldeias and Bicho, 2016; Álvarez et al., 2011; Duarte et al., 2019; Gutiérrez-Zugasti et al., 2011; Mendes Cardoso et al., 2024; Pawłowska and Shillito, 2022; Villagran, 2014), to wood ash and other combustion residues (Marcuzzan et al., 2022; Oikonomou, 2023; Schiegl et al., 2003; Shillito et al., 2011b; Shillito and Matthews, 2013; Starkovich et al., 2020), production residues (e.g. pottery or mudbrick manufacturing, metalworking, cooking) (Brönnimann et al., 2020; Gur-Arieh et al., 2014; Shillito et al., 2011b; Shillito and Matthews, 2013), and/or dung/feces (Brönnimann et al., 2020; Portillo et al., 2019; Shillito et al., 2011a)—middens share a common trait: being sedimentary deposits. Consequently, their geoarchaeological study can yield valuable insights into both the processes and the everyday activities that lead to their formation.

Geoarchaeological studies have revealed the complex processes involved in the formation of midden deposits, notably through the application of high-resolution microcontextual techniques. For instance, Shillito et al. (2011b) and Shillito and Matthews (2013) conducted a microstratigraphic, multi-proxy analysis of the extensive midden deposits at the Neolithic settlement of Çatalhöyük. Their comprehensive approach, integrating archaeological soil micromorphology, inorganic geochemical analysis, lipid biomarker and phytolith analysis, identified a wide range of components in the deposits, including ashes of diverse nature, charred and siliceous plant materials, organic matter, and fecal waste. The study also unveiled various burning activities contributing to the formation of the middens, such as hearth rake-out events and *in situ* burning, utilizing various fuel sources. This provided valuable insights into community distinctions in activities and discard practices within the village. In another study, Brönnimann et al. (2020) examined the sedimentary fills of ditches and pits at the Iron Age site of Basel-Gasfabrik using archaeological soil micromorphology. They identified different functionalities of these features within the settlement, such as water canals and secondary use as roofed constructions for handicraft. This classification was based on various categories of microscopic waste documented, including dung, pottery fragments, animal bone, and charred plant matter, offering insights into the daily life practices in different areas of the settlement.

These cases highlight the key role of geoarchaeology, and particularly of microstratigraphic and microcontextual approaches, in understanding the complex formation processes of middens over time. This is particularly relevant when seeking to infer cultural interpretations based on the archaeological field data recovered from such deposits (Schiffer, 1983), as it becomes crucial to determine their genesis, nature

and degree of integrity.

1.2. Case study: Cerro de San Vicente

Cerro de San Vicente (henceforth CSV) is an Early Iron Age settlement site (ca. 900–400 BCE) located in the Central Iberian Plateau, in the city of Salamanca, Spain (Fig. 1A). Perched at an elevation of 805 masl on a flat-topped hill, the site was discovered in 1951 and has undergone intermittent excavation since 1990 (Blanco-González et al., 2017; Macarro Alcalde and Alario García, 2021). Excavations between 2006 and 2022 have unveiled a 600 m² area corresponding to the late occupation phase of the village, dated through archaeomagnetism to 650 and 570 BCE (with pTRM-check corrected data) (García-Redondo et al., 2021). Within this area, several earthen dwellings have been exposed (Fig. 1B), comprising five roundhouses, two rectangular buildings, and thirteen smaller rounded structures, interpreted as the foundations of storage facilities. Remarkably, field observations suggest that all the buildings were carefully emptied before their abandonment (Blanco-González et al., 2023a, 2022), therefore, hampering the finding of *de facto* refuse—i.e., leaving behind no archaeological artifacts *in situ*, in their systemic or utilitarian context (Schiffer, 1972). Interspersed among these earthen dwellings, ashy, archaeologically-rich deposits have been documented, interpreted in the field as middens and open-air transit areas within the village (Fig. 1C) (Blanco-González et al., 2017).

Overall, the exhumated sector has been interpreted as part of a multi-family courtyard around a central open area, dwelled and shared by an extended household group (Blanco-González et al., 2023a). Its rich and heterogeneous archaeological record—including abundant consumed bones, querns, imported fine tableware and liturgical items—point towards the recurrent performance of social, ritual and crafting activities, such as cooking, grinding and pottery manufacturing (Blanco-González et al., 2023b, 2022).

In a previous study (Tomé et al., 2024), high-resolution micro-contextual geoarchaeological analyses were conducted on three earthen buildings from this area: House 1, House 2, and its Ancillary Structure—a likely storage facility. This study utilized a combination of archaeological soil micromorphology, lipid biomarker analysis, X-Ray fluorescence (XRF), and X-Ray diffraction (XRD). This approach allowed Tomé et al. (2024) to investigate the earthen floor deposits inside the dwellings, revealing various construction layers that formed complex sequences of recurrent cycles of floor use, renovation, and decay. While a few activity layers were identified, micromorphological observations indicated that the dwellings were meticulously maintained over time, likely involving recurrent sweeping and the potential use of mats for floor protection. Lipid biomarkers from the three floor sequences led the authors to conclude that these molecular traces were associated with the past functionality and daily use of the dwellings. However, the identified lipids did not provide sufficient diagnostic information to assess how the buildings were used by their inhabitants, leaving the specific actions performed in the dwellings as an open question.

While the midden deposits outside the dwellings have not yet been studied using this microcontextual geoarchaeological approach, they show great promise for such analyses. As opposed to the roundhouses, the middens have yielded the highest number of archaeological remains. Even though their formation processes are probably linked to the disposal of secondary refuse, preliminary field observations indicate visible absence of post-depositional removal, mixing or truncation of the deposit, therefore supporting their potential stratigraphic integrity (Blanco-González et al., 2017). Based on field data, the current working hypothesis posits that these middens were formed through wood ash dumping. For instance, zooarchaeological data indicates the disposal of both burnt and fresh animal bones in the middens, as evidenced by the presence of bone fragments in different charring states (Blanco-González et al., 2022). The dumped wood ash, along with the residues they contain (e.g. potsherds, fauna and charcoal remains), are believed to have originated from burning activities conducted in the central clay

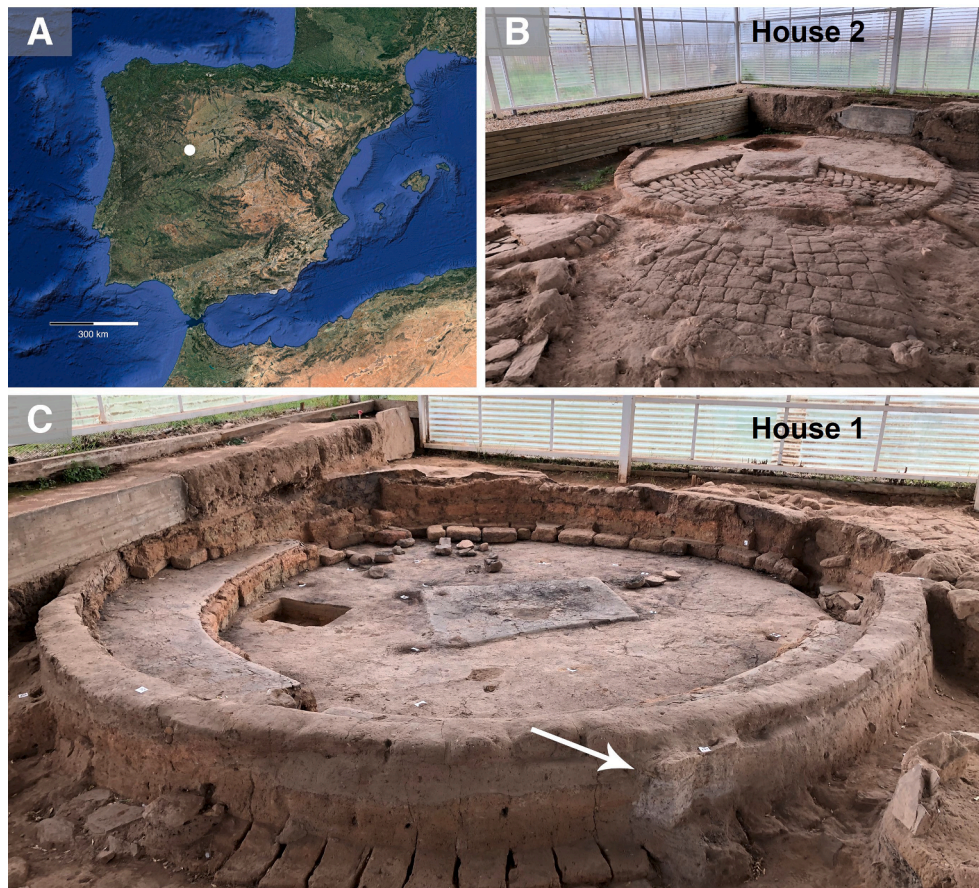


Fig. 1. A) Geographic location of Cerro de San Vicente in the Central Iberian Plateau (white dot). B) Partial view of the excavation surface, showing one of the partially excavated roundhouses of the village (House 2). The diameter of the house is approximately 6.5 m. There is a sedimentary midden deposit (Midden 2) not visible in the image but included in this study, situated east (downward) at the bottom right corner of the image. Noteworthy is the overall good preservation of the dwelling remains, constructed on mudbrick and earthen clay floors. C) Photograph of House 1 (of the same diameter as House 2) displaying a circular bench and a central hearth. The white arrow points to another midden deposit (Midden 1), which rests against the exterior wall of the house.

hearths documented inside the roundhouses. Therefore, if confirmed, these midden deposits could offer vital insights into the household activities conducted within the dwellings and the practices related to pyrotechnology (e.g. fuel sources, fire functionality), waste management, and resource utilization.

Nevertheless, significant specific research questions persist, demanding further exploration and elucidation: Are the midden deposits predominantly composed of wood ash, or do other sedimentary elements contribute to their formation? Did the middens result from a single dumping event or represent long-term accumulations of discarded material? Was there a midden specific to each roundhouse, or are they communal discard areas shared by multiple structures? Lastly, were these middens solely used for discard accumulation, or do they exhibit evidence of other activities, such as crafting, or hosting *in situ* burning events?

As the geoarchaeological study of middens has proven to be a crucial tool for understanding their formation processes and the subsequent inference of cultural interpretations (see section 1.1.), this paper investigates two midden sequences from CSV applying a microcontextual geoarchaeological approach. We coupled archaeological soil micromorphology, sedimentary lipid biomarker analysis, mineralogical (XRD), elemental geochemical (XRF), and magnetic properties analyses to study the midden deposits associated with the dwellings previously examined by Tomé et al. (2024), specifically those adjacent to House 1, House 2 and its Ancillary Structure. Our main aims are to: 1) study midden formation processes; 2) determine the differences and similarities between the two targeted sequences; 3) address daily life practices,

fire use, and waste management in the village; and 4) assess if there are any diachronic and/or spatial patterns and/or changes in discard dumping practices.

2. Materials and methods

2.1. Archaeological soil micromorphology

Two intact and oriented sediment blocks were collected from different sections of the transit area between the dwellings. Block 1 was collected adjacent to House 1 (Midden 1), while Block 2 (Midden 2) was obtained from the deposit situated in front of House 2 and its Ancillary Structure (see Fig. 2). For Block 1, 4 large-sized thin sections (14 cm x 6 cm x 30 μm) were manufactured at the Spanish National Research Center for Human Evolution-CENIEH (Burgos, Spain). For Block 2, two smaller thin sections (4 cm x 3 cm x 30 μm) were produced at Wagner Petrographic Inc. (Utah, USA). The micromorphological analyses were conducted using two petrographic microscopes available in the Archaeological Micromorphology and Biomarkers Lab (AMBILAB, Universidad de La Laguna, Tenerife, Spain), a Nikon E600-POL and a Nikon AZ100 (with epifluorescence module). At the International Center for Archaeology and the Evolution of Human Behaviour (ICArEHB, Universidade do Algarve, Faro, Portugal), a Nikon LV100ND was also used. Microphotographs were taken using a Nikon DS-Ri2 camera, both at AMBILAB and ICArEHB.

Thin section description and interpretation adhered to the standard guidelines provided by Stoops (2003) and Nicosia and Stoops (2017).

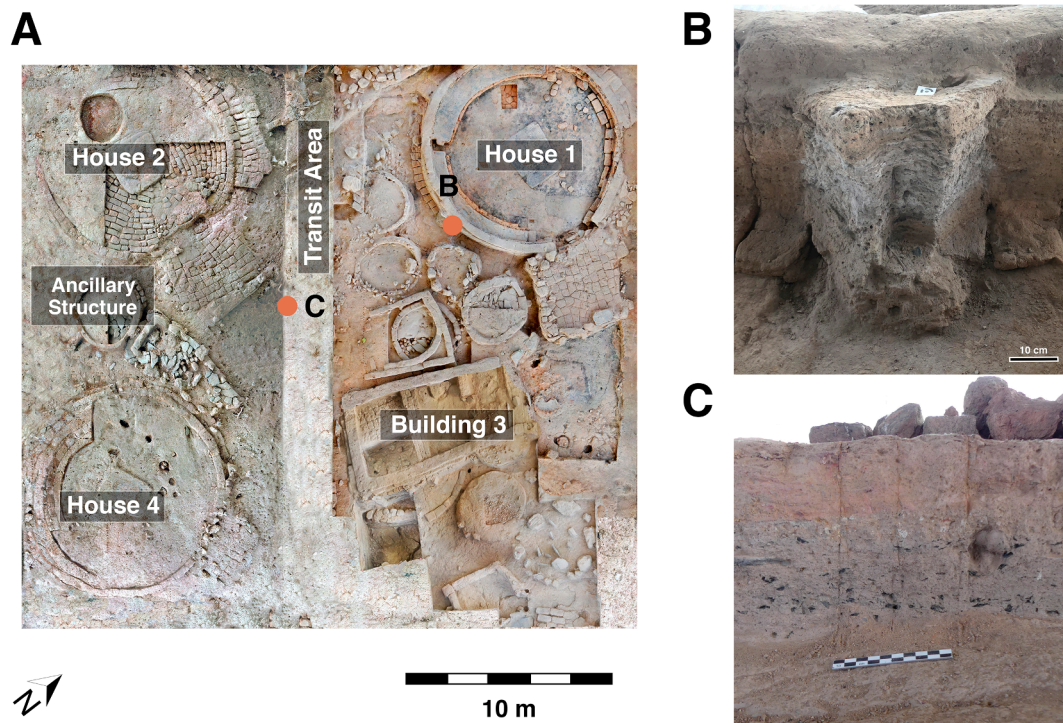


Fig. 2. A) Plan view of the 400 m² sector excavated in 2006–2022, illustrating earthen dwellings and the midden deposits interspersed between them (Transit Area). The orange dots (B and C) represent the spots targeted in this study. B) Stratigraphic sequence of the midden deposit associated with House 1 (Midden 1). Three distinct macroscopic units are observed: a brown silty-clayey deposit at the base, a greyish, silty charcoal-rich deposit in the middle, and a light brown silty-clayey deposit at the top. C) Stratigraphic sequence of the midden deposit associated with House 2 (Midden 2). The deposit exhibits a visible separation into two macroscopic units: a grey, charcoal-rich deposit at the bottom, and a compact, reddish silty-clayey deposit on top.

We applied the concept of microfacies unit (MFU), and utilized the Microfacies Type (MFT) approach to categorize microfacies exhibiting similar and recurrent micromorphological characteristics (Courty, 2001; Goldberg et al., 2009). This approach aims to enhance our understanding and interpretation of site formation processes by identifying specific combinations of micromorphological features throughout the sequences.

2.1.1. Phytolith analysis

Phytolith analysis on thin sections was performed to explore distribution patterns and the taxonomic origin of the biogenic silica. Phytoliths were only observed in the thin sections from Midden 2. The remaining thin sections from Midden 1 were too thick to observe phytoliths.

Each microfacies unit (MFU) from the Midden 2 sequence was scanned across a horizontal transect at 200x, and consecutively, at 400x magnifications. Phytoliths identified within the scanned area were quantified. The VPC Index and distribution pattern, as established by Vrydaghs and Devos (2018), were employed for phytolith characterization. The naming of phytolith morphotypes follows ICPN 2.0 (ICPT 2019).

2.1.2. Charcoal analysis

Charcoal analysis on thin sections consisted of taxonomic identification based on the cross sections of wood fragments, which were compared with wood anatomy atlases (Schweingruber 1990, Akkemik and Yaman 2012). As the observation was carried out on thin section, it was not possible to review diagnostic features in three wood anatomical sections for each charcoal fragment. This constraint reduced the number of charcoal remains which were potentially identifiable. All the identified fragments were measured in their largest side to classify them according to the categories proposed by Marquer and Otto (2020).

2.2. Lipid biomarkers

For lipid biomarker analysis, 20 bulk sediment samples were collected from the same areas where the micromorphology blocks were taken (Midden 1/House 1 and Midden 2/House 2) (see Fig. 2). In the case of Midden 1, the stratified profile remaining after extraction of the micromorphology block was “micro-excavated” and lipid biomarker samples were collected from each successive visible layer. For Midden 2, an intact and oriented sediment block was taken to the AMBLAB for exclusive lipid biomarker subsampling, where it was also “micro-excavated” in the same way. Both sequences underwent meticulous subsampling, guided by changes in sediment texture, composition, and color. All the samples were collected using nitrile gloves, sterilized metal tools and packed in aluminum foil (to avoid phthalate contamination), and were later stored at –20 °C to prevent bacterial degradation (Brittingham et al., 2017).

The processing of the samples was carried out following the procedure previously employed by Tomé et al. (2024). To extract the Total Lipid Extract (TLE), 5 g of sediment were homogenized using an agate mortar for each sample. Lipids were extracted three times, using a 40 mL 9:1 v/v mixture of dichloromethane (DCM)/methanol (MeOH) under ultrasonic irradiation for 30 min (USC 600th from VWR International, Barcelona, Spain). The extract was centrifuged at 4700 rpm for 10 min (Mega Star 1.6 from VWT International), filtered through pyrolyzed glass wool and finally evaporated at 40 °C using a Nitrogen evaporator (RapidVap® Vertex Evaporator from Labconco, Missouri, USA). The TLE was then fractionated employing a chromatographic column, composed of 1 g of calcined silica gel (70–230 mesh) and 0.1 g of sterilized sand (50–70 mesh). Fractions 1 (*n*-alkanes), 2 (aromatics), 3 (ketones, aldehydes and esters), 4 (alcohols), 5 and 6 (fatty acids and other compounds) were eluted for each sample (Table 1). Then, all the fractions were evaporated under Nitrogen flow and stored at –20 °C until the analysis.

Table 1

Solvents, elution volumes and internal standards employed for extracting the lipid fractions of each sample. The average dead volume (DV) was 1500 μL .

Fraction	Solvents and elution	Internal Standard (IS)
1 <i>n</i> -alkanes	3/8 dead volume (DV) <i>n</i> -Hexane	5 α -androstane
2 aromatics	2 DV 8:2 v/v <i>n</i> -Hexane/DCM	5 α -androstane
3 ketones	2 DV DCM	5 α -androstane
4 alcohols	2 DV 1:1 v/v DCM:EtOAc	5 α -androstane-3 β -ol
5 and 6 fatty acids and other compounds	2 DV MeOH	Methyl C19:0

For fractions 4 (alcohols), 5 and 6 (fatty acids and other compounds), 100 μL of *N*, *O*-Bis(trimethylsilyl)trifluoroacetamide (BSTFA) and trimethylchlorosilane (TCMS) 99:1 v/v was added to obtain trimethylsilyl esters (TMS). The mixture was derivatized at 80 $^{\circ}\text{C}$ and then dried. Before measuring with gas chromatography (GC), all the fractions were reconstituted employing 50 μL of DCM per sample and added the internal standard (IS) to each of them (except for alcohols and fatty acids and other compounds, which were spiked before derivatization), according to the data presented in Table 1.

To determine the compounds present in each sample, an Agilent 7890B gas chromatograph was used, attached to a 59774A single quadrupole (Q) MSD with an electron impact interface and equipped with an automatic autosampler and a multimode injector (Agilent Technologies, Waldbronn, Germany). The MassHunter Workstation Software was used to control the system, as well as to acquire and process the data. The equipment conditions for *n*-alkanes were similar to the ones described by Herrera-Herrera et al. (2020), and for aromatics, ketones, alcohols, fatty acids and other compounds, as shown by Tomé et al. (2022). A more detailed description is presented in supplementary material (S1).

Lipid compounds were identified by comparison of the retention times and using the NIST Mass Spectrum Library. *n*-Alkane quantification was accomplished through the utilization of calibration curves generated by plotting the Area/AreaIS ratio against the concentration of reference standards. Additionally, for quantification purposes, the four most prominent fragment ions were selected from the mass spectra (m/z 43, 57, 71, and 85 for *n*-alkanes; m/z 67, 81, 95, and 245 for the internal standard, IS). Concentrations for compounds other than *n*-alkanes were estimated by comparing their area with that of the internal standard (IS). The concentrations are reported in micrograms per gram of dried sample ($\mu\text{g/gds}$) for *n*-alkanes, and in nanograms per gram of dried sample (ng/gds) for other compounds.

In order to ease the interpretation of *n*-alkane data, two indexes were calculated employing the *n*-alkane quantifications obtained through calibration curves (see supplementary material, S2): 1) OEP ($n_{\text{C}27-n_{\text{C}33}}$) (odd-over-even predominance), for establishing the preservation degree of organic matter (Hoefs et al., 2002), and 2) ACL ($n_{\text{C}25-n_{\text{C}33}}$) (average chain length), the weighted average of the various lengths of the carbon chain, aimed at evaluating the main features of the biomass (Freeman and Pancost, 2014; Poynter and Eglinton 1990).

2.3. Mineralogical (XRD) and elemental geochemical (XRF) analyses

For this study, 24 bulk sediment samples were collected from the two midden sequences targeted in this study (Midden 1 and Midden 2) (see Fig. 2). To determine the mineralogical and elemental composition of the sediments, X-ray diffraction (XRD) and X-ray fluorescence (XRF) semiquantitative analyses were conducted on the bulk sediment samples at the I+D+i Scientific-Technological Center of the University of Burgos (Spain).

For mineralogical analysis (XRD), samples underwent careful dry-cleaning and powdering using an agate mortar. Semiquantitative (% weight) mineralogical analysis was performed using a Bruker D8 Advance diffractometer. Diffractogram interpretation and mineral identification employed the DRIFACplus basic EVA software, with a set

limit of detection at 1 % wt. For elemental geochemical analysis (XRF), sediment samples were powdered, homogenized, and mixed with flux (Lithium Metaborate/Tetraborate, 0.5 % KBr), then transformed into beads using an Equilab F1 Induction fluxer. Semiquantitative (% weight) analysis of the samples was conducted with a Thermo ARL ADVAT XP Sequential XRF spectrometer. The XRF equipment had a limit of detection of 0.01 % wt, but only data for major elements well above 1 % wt were considered. Data interpretation employed WinXRF.ADVANT 3.2.1 and UNIQANT v.5.47 software packages.

A Principal Component Analysis (PCA) was performed on the geochemical data. The geochemical data was normalized to Z-scores to avoid scaling effects and to obtain average-centered distributions. PCA was performed with SPSS 28.0 software to reduce the number of variables to a set of Principal Components (PCs), representative of groups of features following similar trends. Rotated (Varimax) and non-rotated solutions were evaluated, and the most suitable one to the geochemical data variance was selected.

2.4. Magnetic properties

Magnetic susceptibility was measured on 21 bulk (unoriented) samples collected from the 40 cm-thick sequence of Midden 1. The sampling resolution was 1 sample per 2 cm. Magnetic susceptibility was measured with a KLY-4 susceptibility bridge (average of three measurements) and corrected on a mass specific basis. In addition, on 4 representative samples of the different facies identified, several experiments were carried out to characterize their composition (type of ferromagnetic mineral/s), concentration and grain size. These experiments comprised progressive isothermal remanent magnetisation (IRM) acquisition curves, hysteresis cycles (± 1 T), backfield coercivity curves and thermomagnetic curves (magnetization vs temperature) up to 700 $^{\circ}\text{C}$ in air. All these experiments were performed with a variable magnetic field translation balance (MM_VFTB) at the Laboratory of Paleomagnetism of Burgos University (Spain).

3. Results

3.1. Archaeological soil micromorphology

3.1.1. Lithology, microstructure, and main components

The Midden 1 and Midden 2 sequences exhibit a homogeneous lithological composition, primarily comprising terrigenous, siliciclastic sediments with abundant angular and subangular quartz grains ranging between silt and gravel. Additionally, gravel and sand-sized angular and subangular slate and quartzite fragments, along with silt-sized to sand-sized mica-group minerals, were recurrently identified. A more detailed description of the lithological composition of each sample is presented in supplementary material (S3).

The most prevalent microstructures in Midden 1 are massive and complex (at the bottom and the upper part of the sequence), whereas spongy/platy is documented in the middle section of the sequence. In Midden 2, massive and complex microstructures are consistently present throughout the sequence, and intergrain microaggregate has been occasionally identified. Overall, both sequences predominantly exhibit a porphyric c/f related distribution. Bioturbation features are moderately

Table 2

Description of the main components identified in the micromorphological samples. Microphotographs of each component are presented in Fig. 3. To identify the specific location and abundance of the components in each sample, see supplementary material (S3).

Component	Description	Significance
Charcoal	Very abundant Sand to gravel-sized Rounded and subrounded Mostly well-preserved, with intact inner cell structure	Wood burning
Charred plant material	Very abundant Coarse silt-sized and fine sand-sized Some rounded, unidentified Sometimes fine and elongated, resembling chaff	Plant burning. Implies low burning temperatures
Calcitic wood ash	Very abundant Reworked (as sand-sized aggregates) with clay and silt-to-sand-sized quartz and mica grains and sand-sized earth-based construction material fragments; or massive, displaying a spongy/platy microstructure Calcium oxalate crystals	Wood burning activity. Implies high burning temperatures
Animal bone	Abundant Subangular and angular, predominantly sand-sized Yellow (likely unburnt), or brown/dark orange (likely burnt) Few light grey, calcined fragments Good preservation states; a few fissured fragments	Suggests waste from cooking/consumption of animal products and/or other activities, such as animal skin removal
Organic tissue	Few Fine to coarse sand-sized Light orange Diffusely bedded	Indicates presence of fresh plant tissue
Earth-based construction materials	Abundant in the upper sequence of Midden 2 Also documented throughout the Midden 1 sequence Usually displayed as 1) sand to gravel-sized anorthic clay nodules with sharp boundaries; they contain clay coated quartz sand grains (~60%), 2) sand to gravel-sized disorthic dark-brown clay nodules, with mica-type minerals and fine sand-sized quartz (~20–35%)	Suggests discard of earth-based construction materials

present in both sequences. These mainly consist of calcium carbonate hypocoatings on channels and chambers, granotubules, and occasionally a channel porosity associated with fresh organic tissue and recent root fragments. A more detailed description of these micromorphological features per sample is presented in [supplementary material \(S3\)](#).

Anthropogenic components are abundant and consistently documented throughout the sequences. These components primarily include calcitic wood ash, charcoal, silt-sized unidentified charred plant matter, organic tissue, yellow and orange bone fragments, and earth-based construction materials. A more detailed and comprehensive description of these components is provided in [Table 2](#) and [Fig. 3](#). To identify the specific location of the components in each sample, see [supplementary material \(S3\)](#).

3.1.2. Microfacies units (MFU) and microfacies types (MFT)

According to the features outlined in [Section 3.1.1](#), we have identified 20 microfacies units (MFU) in Midden 1 and 10 MFU in Midden 2. These MFU are correlated with 20 biomarker samples (see [Fig. 4](#), [supplementary material S3](#)). In order to enhance the interpretation of the sequences, these MFU have been categorized into 6 microfacies types (MFT). These add up to the earlier MFT documented by [Tomé et al. \(2024\)](#) at CSV (see [supplementary material S4](#)), bringing the total number of MFT documented at the site to 11. Overall, we have identified the recurring presence of three main types of microfacies: 1) silty/sandy-clayey deposits of terrigenous siliciclastic sediments, mixed with calcitic wood ash, other combustion residues (charcoal, silt-sized charred plant matter) and earth-based construction material fragments (MFT 6, MFT 7, MFT 8); 2) massive deposits of intact, heterogeneous earth based-construction material fragments (MFT 9); and 3) compact, diffusely bedded deposits of calcitic wood ash with variable amounts of other combustion residues and organic dust (MFT 10 and MFT 11). Their detailed descriptions are provided in [Table 3](#) and [Fig. 5](#).

3.1.3. Phytolith analysis

The distribution pattern of phytoliths has been quantitatively recorded in Midden 2, across MFU 1 to 10 (see [supplementary material, S5](#)). The quantification of the identified phytolith morphotypes is shown

in [supplementary material \(S6\)](#). Overall, monocot and grass phytoliths are the most abundant, particularly morphotypes such as ELONGATE ENTIRE, ELONGATE SINUATE, ELONGATE DENTATE and RONDEL. [Fig. 6](#) shows the relative abundance of monocot vs dicot and inflorescence vs leaf/stem phytoliths.

3.1.4. Charcoal analysis

A total of 40 charcoal samples were taxonomically identified: 18 from the thin sections of Midden 1 and 22 from Midden 2 ([supplementary material, S7](#)). In Midden 1, the identified charcoal pieces range in size from 5 mm to 0.3 mm, with 17 being classified as charcoal pieces and one as a fragment, according to the classification established by [Marquer and Otto \(2020\)](#). In Midden 2, the charcoal samples are smaller, ranging from 4 mm to 0.4 mm, with 21 classified as charcoal pieces and one as a fragment ([supplementary material, S7](#)).

The taxonomic composition shows differences between the sequences. In Midden 1, 4 taxa were identified –evergreen and deciduous *Quercus*, *Quercus* sp. and dicot–, whilst 5 taxa have been identified in Midden 2 –evergreen and deciduous *Quercus*, *Quercus* sp., *Pinus* sp., and Coniferae– ([Fig. 7](#), [supplementary material S7](#)).

3.2. Lipid biomarkers

3.2.1. *n*-Alkanes

n-Alkanes were detected, identified and quantified in the 20 bulk sediment samples. In Midden 1, *n*-alkanes range from *n*-C₁₈ to *n*-C₃₃, and their total concentration oscillates between 0.01 and 0.07 µg/gds. In Midden 2, the distribution varies from *n*-C₁₈ to *n*-C₃₅, and the overall *n*-alkane concentration per sample ranges between 0.06 and 0.07 µg/gds. The predominant *n*-alkanes in both sequences are *n*-C₂₉, *n*-C₃₁ and *n*-C₃₃. Notably, the *n*-alkane profiles exhibit a smoothed, odd-over-even distribution ([Fig. 8](#), [supplementary material S8 and S9](#)).

n-Alkane indexes OEP and ACL were calculated for all the samples (see [supplementary material S2 and S9](#)). In Midden 1, OEP ranges from 1.38 to 8.08, and ACL between 28.96 and 30.82. In Midden 2, OEP values oscillate between 2.82 and 3.82, and ACL ranges from 29.00 and 29.72.

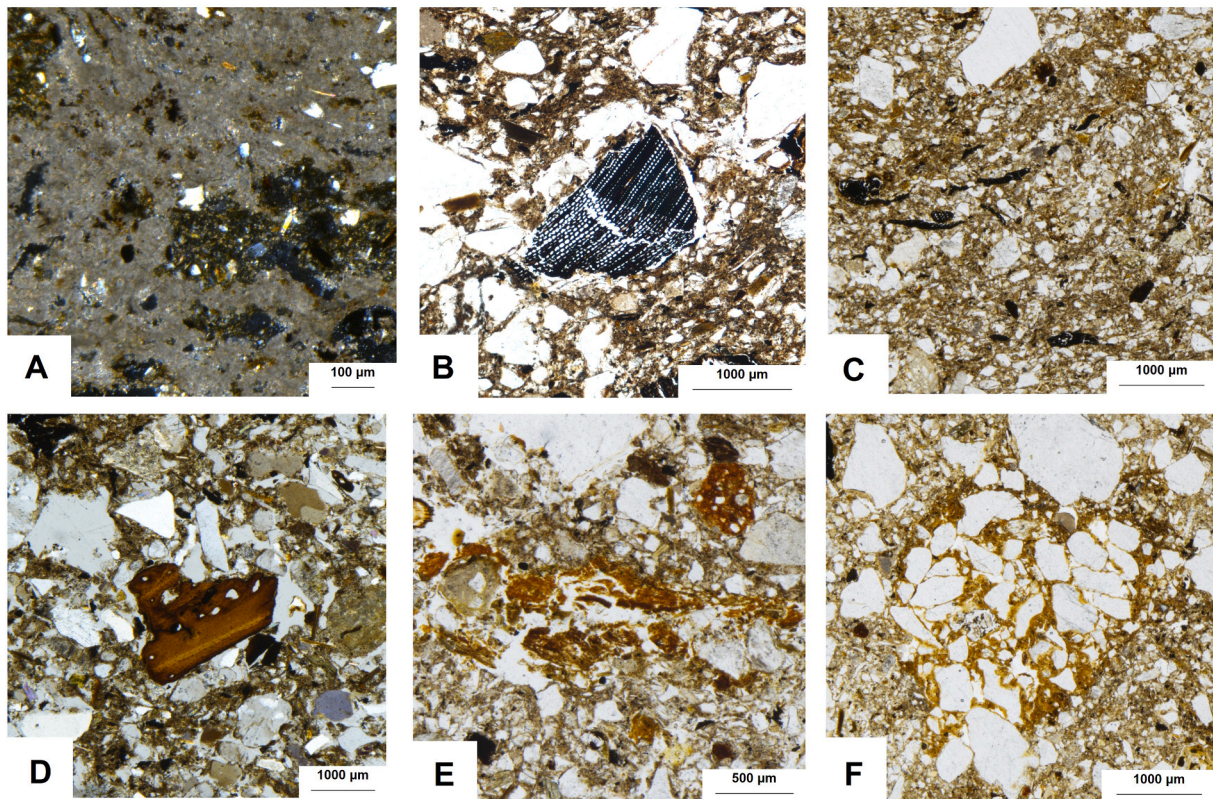


Fig. 3. Microphotographs (PPL, unless stated otherwise) of the most prevalent microscopic anthropogenic components identified in the midden deposits. A more detailed description of these components is provided in [Table 2](#). **A)** XPL. Calcitic-crystallitic wood ash with charcoal and earth-based construction material inclusions. It is highly abundant in both Midden 1 and Midden 2. It has been observed in a massive and spongy/platy microstructure, as well as in reworked subrounded aggregates. **B)** Charcoal. It is found in different sizes and variably angular to subrounded depending on the particular context. It is very abundant in both sequences and overall exhibits excellent preservation. **C)** Silt and sand-sized unidentified charred plant matter. It is very abundant in both sequences, and it exhibits either rounded or elongated shapes. **D)** Animal bone. It is documented in both sequences and typically exhibits a subangular/angular shape and a dark orange/brown color, suggesting burning. Additionally, it has been observed in a light pale-yellow color. **E)** Unburnt tissue. It is occasionally documented in Midden 2, *in situ* and bedded, particularly in the lower section of the sequence. **F)** Earth-based construction material fragments. It is abundant in the upper sequence of Midden 2, and it is also occasionally documented throughout Midden 1. It is usually displayed as anorthic nodules with sharp boundaries and quartz sand in a clayey matrix, as displayed in the microphotograph.

3.2.2. Other compounds

Other compounds, including ketones, alcohols, fatty acids and terpenoids, were detected and identified in the 20 bulk sediment samples, and their concentrations were subsequently estimated. Ketones were exclusively identified in the sequence of Midden 2, including 2-pentadecanone and 2-octadecanone. *n*-Alkanols range from C₁₁-OH to C₁₈-OH, with a predominant presence in Midden 1. In both Midden 1 and Midden 2, fatty acids range from C_{9:0} to C_{24:0}, with C_{16:0} and C_{18:0} being the most recurrent and abundant overall. Oleic acid was also occasionally identified in Midden 1, and cholesterol was detected in Midden 2. In addition, triterpenoids friedelan-3-one and friedeline were solely documented in Midden 2. In both Midden 1 and Midden 2, diterpenoid dehydroabietic acid was identified. For a more detailed and comprehensive overview of the identified compounds in each of the samples and their estimated concentrations, see [supplementary material \(S10\)](#).

3.3. Mineralogical (XRD) and elemental geochemical (XRF) analyses

XRD analysis shows mineralogical variability in the sediment samples from Midden 1 and Midden 2, mainly consisting of siliceous minerals: quartz, clay minerals, feldspars, and carbonate minerals (calcite). The analyzed samples present more silicate minerals at the top and the bottom of the studied sequences and vary gradually towards the central part, where calcite is the most abundant mineral ([Fig. 9, supplementary material S11](#)). In this sense, quartz proportions range from 53.68 % to 4.73 % wt, clay minerals from 35.39 % to 2.09 % wt, feldspars from

42.39 % to 2.57 % wt and calcite from 71.34 % to 1.92 % wt.

Elemental geochemical composition analysis (XRF) also yielded a variable distribution, showing an increase of silicate-related elements at the bottom and the top of the sequences. SiO₂ is the predominant compound in siliceous samples (between 69.44 % and 20.7 % wt), followed by Al₂O₃ (from 13.63 % to 5.13 % wt) and Fe₂O₃ (between 4.45 % and 1.5 % wt). In the middle of the sequence of Midden 1, CaO is the most common compound, ranging between 3.27 % and 60.78 % wt. The presence of K₂O, Na₂O, MgO, TiO₂, Br and P₂O₅ was also documented, but in lower proportions (less than 3 %) ([supplementary material, S12](#)). A single principal component explains most of their variability (86.14 %). Silicate-sediment related elements (SiO₂, Al₂O₃, etc.) vary inversely to calcium (CaO) and phosphate (P₂O₅) ([supplementary material, S13](#)).

3.4. Magnetic properties

From top to bottom, the magnetic susceptibility (MS) profile of Midden 1 exhibits a progressive increase to a maximum value around 22 cm of depth. From there downwards, there is a progressive trend towards decreasing MS. The highest MS values correspond to the central part of the sequence, associated with MFT 10 and MFT11 (ash-rich layers), while the lowest values, identified both at the top and bottom of the sequence, are linked to MFT 6 (earth-based construction material-rich layers). Rock-magnetic experiments performed on representative samples from the central part (e.g. sample 22) indicate that the magnetization carrier is magnetite (Curie temperature or TC=580 °C)

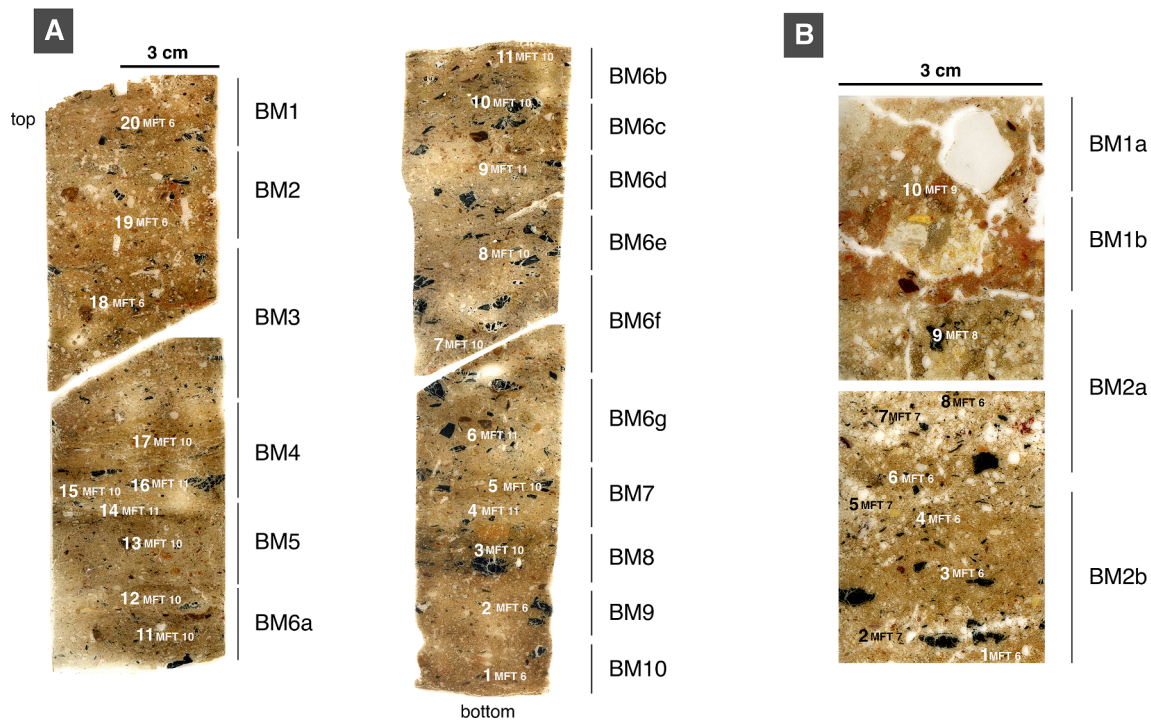


Fig. 4. Thin section scans of the midden sequences, including microfacies units (MFU) (white numbers), microfacies types (MFT), and associated biomarker samples (BM). A) Midden 1 B) Midden 2.

(Dunlop and Özdemir, 1997). Their IRM acquisition curves saturate around 150–200 mT, are highly magnetic samples and their thermomagnetic curves are reversible up to 700 °C (coincidence between heating and cooling cycles), indicating that these samples originally reached this temperature (supplementary material S14A-B). Alternatively, samples corresponding to the top (sample 36) and bottom (0) indicate that, in addition to magnetite and/or maghemite (TC of 580 °C or slightly over), there is also haematite. They are also highly magnetic samples, but their IRM curves are not completely saturated indicating the coexistence of a high coercivity mineral (supplementary material S14C-D). It is haematite, identified in the thermomagnetic curves with TC of 675 °C. This would explain the lower MS values identified in these samples, as identified in micromorphological analysis, contain abundant earth-based construction material fragments. The thermomagnetic curve of sample CSV2-0 (base of the sequence) is fully reversible indicating that it originally reached 700 °C (supplementary material S14D). On the contrary, the thermomagnetic curve of sample CSV2-36 (top of the sequence) is very magnetic but not reversible at 700 °C. Since no magneto-mineralogical transformations are observed in its heating cycle, this sample was most probably heated between 400 and 700 °C.

4. Discussion

The microcontextual geoarchaeological study of the midden sequences at CSV has allowed us to identify and characterize their formation processes. These deposits exhibit multiple, complex microstratified layers. Three main deposit types have been identified based on their micromorphological features. Two of them contain earth-based construction materials, one of these with wood ash (MFT 6, MFT 7) and one without (MFT 9), and a third type is composed exclusively of compact beds of wood ash and other combustion residues (MFT 10, MFT 11). In both Midden 1 and Midden 2 the lipid record has been preserved, including *n*-alkanes, *n*-alkanols, fatty acids and terpenoids, particularly angiosperm and gymnosperm-specific compounds. The *n*-alkane record shows an overall smoothed odd-over-even predominance, suggesting organic matter burning. Additionally, we have identified, on thin

section, the presence of *Quercus* sp., *Pinus* sp., Coniferae and dicot charcoal fragments, as well as the predominant presence of monocot phytoliths in Midden 2.

In the subsequent paragraphs, we discuss the data obtained, integrate it with the existing microcontextual geoarchaeological dataset of CSV (Tomé et al., 2024), and explore its archaeological significance in shaping our understanding of formation processes, daily life practices and space use within the village.

4.1. The disposal and disintegration of earth-based construction materials

In Midden 1 and Midden 2, we have identified the presence of compact, silty-clayey, grano-striated deposits of terrigenous siliciclastic sediments mixed with reworked wood ash (MFT 6, MFT 7 and MFT 8) (Fig. 5, Table 3). They also contain components such as charcoal, silt-sized charred plant matter, bone (burnt and unburnt), fresh organic tissue and fragments of earth-based construction materials. These deposits may exhibit fine horizontal bedding and horizontal orientation of the coarse components. The overall micromass features bear significant resemblance to those previously identified within CSV by Tomé et al. (2024), particularly in earth-based silty-clayey construction floors (MFT 2) and mudbrick (MFT 5). The mineralogical and elemental geochemical composition of these deposits also exhibits similarities with data obtained from such earth-based construction floors, showing the abundance of quartz, clay minerals and feldspars, and SiO₂, Al₂O₃ and Fe₂O₃ (Tomé et al. 2024). Their grano-striated b-fabric, the presence of fine bedding and the mixture of the micromass with earth-based construction material fragments, in the form of disorthic and anorthic nodules, suggest that these deposits were likely formed through the disintegration, dispersion and degradation of earth-based construction materials, including both adobe and earth-based construction floors (MFT 2, MFT 5) (Friesem et al., 2011, 2014; Goodman-Elgar, 2008; Gutiérrez-Rodríguez et al., 2022). The identification of horizontal parallel diffuse bedding and the degree of compaction suggests recurrent anthropogenic trampling and foot traffic (Lisá et al., 2020; Rentzel et al., 2017) (Fig. 10A). During this process, the earth-based construction materials

Table 3

Microfacies types (MFT) identified in the micromorphological samples and their correlation with Microfacies Units (MFU) ($c/f_{63\mu m}$). These MFT add up to the earlier MFT documented by Tomé et al. (2024) at Cerro de San Vicente (see supplementary material, S4). Microphotographs of each MFT are presented in Fig. 6.

Microfacies Type	Description	Deposit Type	Microfacies Unit
6	Massive, compact, with a light brown silty-clayey grano-striated micromass (55–65 %) and variable amounts of calcitic-crystallitic wood ash (5–20 %) Abundant combustion-derived components, animal bone fragments and sand-sized earth-based construction material fragments (disorthic nodules) Thickness: 1 cm – 4 cm Lithology: angular coarse silt-sized to fine sand-sized mica-group minerals (10–20 %), subangular fine-to-medium sand-sized quartz (10–15 %), subangular sand-sized slate (5–10 %)	Midden	Midden 1: 1, 2, 15, 18, 19, 20 Midden 2: 1, 3, 4, 6, 8
7	Intergain microaggregate, loose deposit with light brown silty-clayey grano-striated micromass (15–30 %), calcitic-crystallitic wood ash (5–10 %) Abundant combustion-derived components and animal bone fragments Thickness: 0.5 cm – 1 cm Lithology: angular coarse silt-sized to fine sand-sized mica-group minerals (10–20 %), subangular coarse sand-sized quartz and quartzite (15–25 %), subangular sand-sized slate (5 %)	Midden	Midden 2: 2, 5, 7
8	Massive, compact light-yellow silty-clayey micromass (40–60 %), calcitic-crystallitic wood ash (~5%) with organic silt Abundant combustion-derived components and sand-sized, subrounded earth-based construction material fragments (disorthic and anorthic nodules) Thickness: 2 cm Lithology: angular coarse silt-sized to fine sand-sized mica-group minerals (10–20 %), subangular coarse-to-medium sand-sized quartz and quartzite (10–15 %), subangular sand-sized slate (~5%)	Midden	Midden 2: 9
9	Massive, compact deposit of heterogeneous silty-clayey micromass (50–65 %) Abundant sand-sized, subrounded and subangular earth-based construction material fragments (disorthic and anorthic nodules) Thickness: 4 cm Lithology: angular coarse silt-sized to fine sand-sized mica-group minerals (10–20 %), subangular coarse-to-medium sand-sized quartz and quartzite (15–20 %), subangular sand-sized slate (~5%)	Accumulation of construction material	Midden 2: 10
10	Massive, compact deposit of calcitic-crystallitic, silty micromass (50–65 %), with organic silt (15–25 %). Diffuse horizontal bedding Abundant combustion-derived components, subangular animal bone fragments and sand-sized subrounded earth-based construction material fragments (anorthic nodules) Thickness: 1 cm – 3.5 cm Lithology: angular coarse silt-sized to fine sand-sized mica-group minerals (5–10 %), subangular fine-to-medium quartz and quartzite sand (5–10 %), subangular medium sand-sized slate (<5%)	Midden	Midden 1: 3, 5, 7, 8, 10, 11, 12, 13, 17
11	Massive / spongy – platy, compact calcitic-crystallitic silty micromass (70–85 %). Diffuse horizontal bedding Abundant combustion derived components, mostly charcoal and silt-sized charred plant matter, subangular animal bone and sand-sized sand-sized earth-based construction material fragments (anorthic nodules) Thickness: 0.5 cm – 2 cm Lithology: angular coarse silt-sized to fine sand-sized mica-group minerals (~5%), subangular fine-to-medium quartz sand (5–10 %), subangular medium sand-sized slate (~5%),	Midden	Midden 1: 4, 6, 9, 14, 16

were likely mixed with combustion refuse, as evidenced by the presence of subrounded reworked wood ash aggregates.

The abundance of varied anthropogenic components is particularly prominent in the lower-middle section of Midden 2, suggesting that refuse disposal practices also played a key role in the formation processes of the sequence (Shillito, 2015). Both burnt and unburnt bone fragments have been recorded, along with numerous well-preserved charcoal pieces, including *Pinus* sp., *Quercus* sp. *evergreen*, and *Quercus* sp. *deciduous* and other conifer fragments. This points towards heterogeneity in the disposed materials. Lipid biomarker data corroborates this heterogeneity, revealing both conifer-specific compounds (dehydroabietic acid) (Davara et al., 2023; Mackenzie et al., 1982; Oros and Simoneit, 2001a) and compounds associated with angiosperm *input* (friedelan-3-one, friedeline) (Diefendorf et al., 2011; Oros and Simoneit, 2001b), along with the presence of cholesterol. *n*-Alkane data and ACL values, which range between 29 and 29.8, indicate the presence of terrestrial plants, probably involving both woody taxa and grasses (Cranwell, 1973; Diefendorf et al., 2011; Freeman and Pancost, 2014). Phytoliths have also been recorded throughout these microfacies, with an overall predominance of monocots (Fig. 6) likely linked to the presence of grasses, due to the abundance of RONDEL types (Piperno, 2006). Their arrangement, often found in clusters and occasionally articulated, indicates overall good preservation. Therefore, even though these deposits were mainly formed through the disintegration and trampling of earth-based construction materials and refuse disposal, they do not seem

to have been significantly disturbed by anthropogenic, biogenic, or geogenic processes.

The uppermost section of Midden 2, however, exhibits different micromorphological features compared to those described above. It consists of a compact, grano-striated silty-clayey massive deposit of earth-based construction material fragments (MFT 9) (Fig. 4, Table 3), including earthen floor fragments (MFT 2) and fragments of floor preparation surfaces (MFT 1b) (supplementary material, S4) (Fig. 10B), displayed as anorthic nodules with clear, subangular and subrounded sharp boundaries. These earth-based construction fragments remain intact, showing no evidence of post-depositional disturbance. The absence of subhorizontal diffuse bedding, the lack of anthropogenic components (e.g. combustion debris, animal bone fragments) and the decrease in phytolith content suggests that an intentional anthropogenic deposition of earthen construction material resulted in the formation of this layer. However, the reasons behind this hypothetical event remain unclear. Does it represent an accumulation of discarded construction material? Were these fragments deposited there as components of a prepared surface, or for leveling purposes? Whereas constructed layers have been previously documented in other midden contexts, such as those at Çatalhöyük (Matthews, 2005), in the case of Midden 2 from CSV the absence of any overlying anthropogenic components in the upper contact does not allow us to propose any possible past functionality.

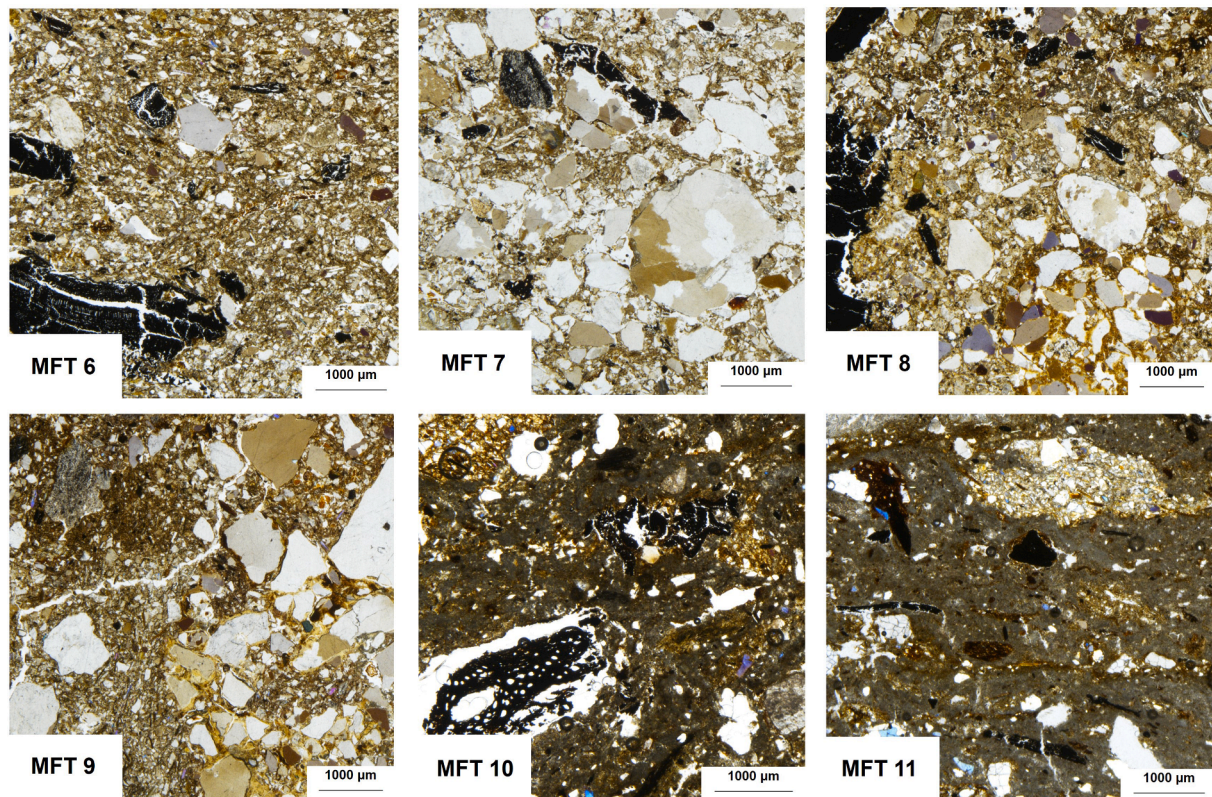


Fig. 5. Microphotographs (PPL) of the Microfacies Type (MFT) identified throughout the micromorphological samples. A detailed description of each type is presented in [Table 3](#). These MFT add up to the MFT documented by [Tomé et al. \(2024\)](#) in the same site (see supplementary material, S4). **MFT 6)** Massive, diffusely bedded brown silty-clayey deposit with reworked calcitic wood ash and medium quartz sand. Subrounded charcoal, subangular animal bone and silt-sized charred plant matter are the most recurrent components. **MFT 7)** Brown silty-clayey deposit with coarse quartz sand, mixed with reworked calcitic wood ash. Subrounded and rounded charcoal is commonly present (sometimes fractured), along with silt-sized charred plant matter. **MFT 8)** Massive deposit, made of light brown silty-clayey sediments mixed with reworked calcitic ash and organic silt. Charcoal and unidentified charred plant matter are abundant, as well as earth-based construction material fragments. **MFT 9)** Massive, heterogeneous deposit, with a brown clayey micromass, coarse quartz and quartzite sand inclusions and abundant disorthic and anorthic nodules (earth-based construction material fragments). **MFT 10)** Massive, spongy deposit composed of calcitic wood ash mixed with silty organic dust. Charcoal and unidentified charred plant matter are abundant, along with fragments of earth-based construction materials and animal bone. **MFT 11)** Massive, spongy deposit of well-preserved, intact calcitic wood ash. It may exhibit secondary ferruginous infillings in some pores, particularly in horizontal planes. There is abundance of charcoal and unidentified charred plant matter, along with fragments of earth-based construction materials and calcined animal bone.

4.2. The ash-rich deposits

In the middle section of the sequence of Midden 1 (MFU 3–MFU 17), a complex succession of calcitic, massive/spongy deposits with platy domains (MFT 10, MFT 11) has been documented. These deposits primarily consist of calcitic wood ash, often appearing articulated and occasionally exhibiting diffuse bedding, with overall good preservation. The elemental geochemical composition of these layers also displays the presence of calcite (CaCO_3), ranging between 60.8 % and 37.8 % ([supplementary material, S12](#)). While MFT 10 represents an organic-rich deposit, with abundant organic dust mixed with calcitic wood ash, MFT 11 consists of pure calcitic wood ash, together with fragments of earth-based construction materials, charcoal, and silt-sized charred plant matter.

The interpretation of the genesis of MFT 11 is complex. Firstly, there are no clear micromorphological features of ash mobilization. This data alone would support, *a priori*, the hypothesis that these layers represent recurrent *in situ* burning events ([Mallol et al., 2017, 2013a; Mentzer, 2014](#)). However, the presence of certain components within the calcitic matrix, and particularly earth-based constructed floor fragments (MFT 2) ([Fig. 10C](#)), suggests that these layers could have formed through recurrent hearth rake-out events ([Mentzer, 2014; Shillito and Matthews, 2013](#)). These constructed floor fragments, most of which do not display burning evidence, would have been incorporated into the ashy matrix through sweeping. The thickness of these microfacies range between 0.5

cm and 2 cm, but these deposits were probably thicker in their original form, prior to compaction, and would thus correspond to multiple ash deposition events ([Karkanas, 2021](#)). These layers would have been compacted through trampling, which is further supported by the presence of diffuse bedding and the horizontal disposition of coarser components ([Rentzel et al., 2017](#)). This, along with the absence of burnt substrates (black/red layers) ([Aldeias et al., 2016; Mallol et al., 2017, 2013b; Mentzer, 2014](#)) throughout the deposit, suggests that these microfacies were formed through recurrent hearth cleaning events ([Mallol et al., 2017; Miller et al., 2010; Schiegl et al., 2003](#)). This is further supported by the archaeological record documented in Midden 1, which included abundant consumed, unburnt animal bone and pottery fragments ([Blanco-González et al., 2022](#)). This interpretation is also consistent with previous micromorphological observations inside House 1, which indicated a scarcity of anthropogenic components, including burning refuse. This scarcity was interpreted as the result of regular, intensive maintenance practices ([Tomé et al. 2024](#)).

On the other hand, MFT 10 (specially, MFU 13 and MFU 17) shows evidence of intense compaction: a massive microstructure with parallel vertical and subhorizontal planes ([Fig. 10D](#)). These features are usually interpreted as signs of trampling ([Mallol et al., 2013a; Rentzel et al., 2017](#)). In addition, the abundant presence of organic debris and other anthropogenic components (e.g. charcoal, burnt and unburnt bone, earth-based construction material fragments), suggests that these microfacies were also deposited because of hearth rake-out activities,

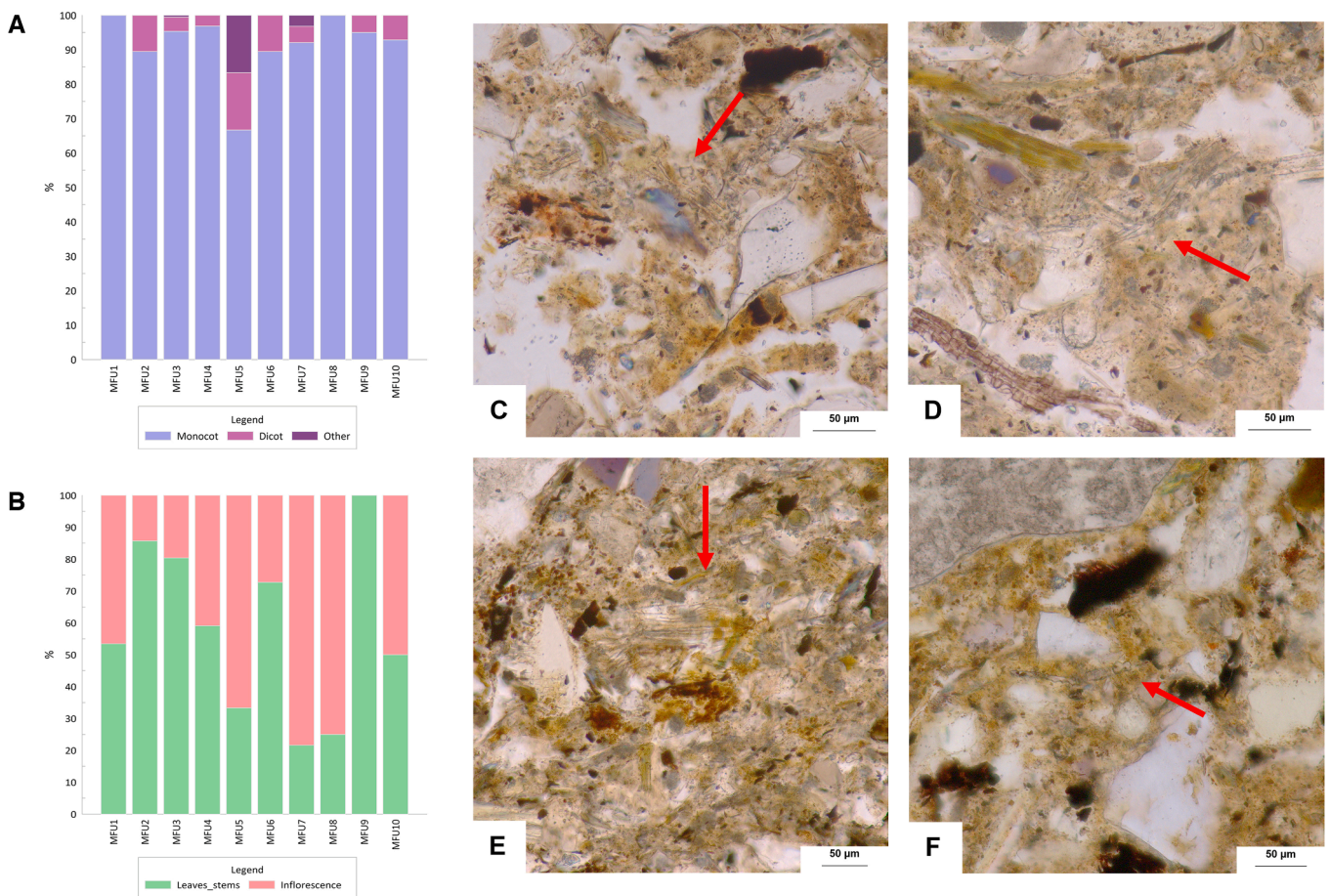


Fig. 6. A) Relative abundance of monocot and dicot phytoliths across the Midden 2 sequence. B) Relative abundance of monocot inflorescence vs leaf/stem phytoliths across Midden 2. C) and D) Clusters of monocot phytoliths; note the abundance of ELONGATE DENTATE morphotypes (VPC=CAA; Moderate visibility, perfect preservation, colorless). E) Cluster of various articulated monocot phytoliths; ELONGATE ENTIRE are dominant (VPC=CAA; Moderate visibility, perfect preservation, colorless). F) Three phytoliths (from left to right: ELONGATE DENTATE, TRAPEZOID or ELONGATE SINUATE, and BILOBATE) forming a small cluster (VPC=BAA; Good visibility, perfect preservation, colorless). VPC labels follow Vrydaghs and Devos (2018).

but were likely exposed for longer periods before the next ash dump event. This would result in compact, organic-rich ashy deposits that were frequently trampled and transited by the village inhabitants. However, the timing and discard rate of these dumping events remain uncertain. The micromorphological characteristics of these layers suggest excellent preservation of the ashy deposits, possibly pointing to a high discard rate. This is further supported by the absence of intense bioturbation (Gutiérrez-Rodríguez et al., 2022; Shillito and Matthews, 2013), despite the occasional presence of channels with calcium carbonate hypocoatings and granotubules (see section 3.1.1), associated with root and insect activity. Considering this, Midden 1 may not have been a fully open-air space, but rather a semi-covered area beneath the roof of House 1, which was likely constructed on earthen materials and wood (Blanco-González et al. 2022). This could explain the absence of ash mobilization or dissolution features and the overall low incidence of bioturbation.

Additionally, organic molecules have been preserved throughout this ash-rich sequence. Lipid biomarker data shows homogeneity in the organic matter content: overall, the samples display a similar *n*-alkane concentration and distribution throughout the deposit (Fig. 8, supplementary material, S8, S9), with a predominance of *n*-C₃₁ and *n*-C₃₃ and a smoothed odd-over-even profile, which is typically associated with organic matter thermal alteration (Fernández-Palacios et al., 2023; Leierer et al., 2019; Tomé et al., 2022; Wiesenberget al., 2009). Fatty acids (from C_{9:0} to C_{20:0}), are recurrently present, with particularly high C_{16:0} and C_{1:08} concentrations (supplementary material, S10). This

suggests that the overall organic matter content and the subsequent rake-out of the hearth refuse were likely homogeneous and consistent over time. In addition, out of the 14 charcoal fragments identified in these microfacies, 13 were identified as *Quercus* sp., with a predominance of *Quercus* sp. evergreen (9) (supplementary material, S7). *Pinus* tp. *pinia/pinaster* and evergreen *Quercus* were predominant amongst the charcoal samples previously analyzed in House 1 (Blanco-González et al. 2022). Pine wood was interpreted to be used as structural timber, and the small twigs of evergreen *Quercus* as lighter structural elements, probably hurdles. However, their presence in Midden 1 suggests their use also as firewood, as it has been recorded in other Iron Age sites from this region (Rubiales et al., 2011).

The molecular data from the earth-based floors of House 1 (Tomé et al. 2024) show similarities with the outside deposit. Both sequences feature *n*-alkanes ranging from *n*-C₂₁ to *n*-C₃₃, with prevailing ACL values between 29.5 and 30. However, whereas the *n*-alkane profiles from House 1 showed no evidence of thermal alteration, the *n*-alkane data from Midden 1 indicates burning activity. Additionally, dehydroabietic acid, a compound linked to conifer *input* (Davara et al., 2023; Mackenzie et al., 1982; Oros and Simoneit, 2001a), was recurrently detected in House 1 and found in the ash-rich deposits of Midden 1. This conifer *input*, detected at a molecular scale, could be associated with the presence of *Pinus* tp. *pinia/pinaster*, which was previously identified through charred wood analysis in House 1 (Blanco-González et al., 2022). Furthermore, oleic acid and mid and long-chain fatty acids were also documented in both sequences.

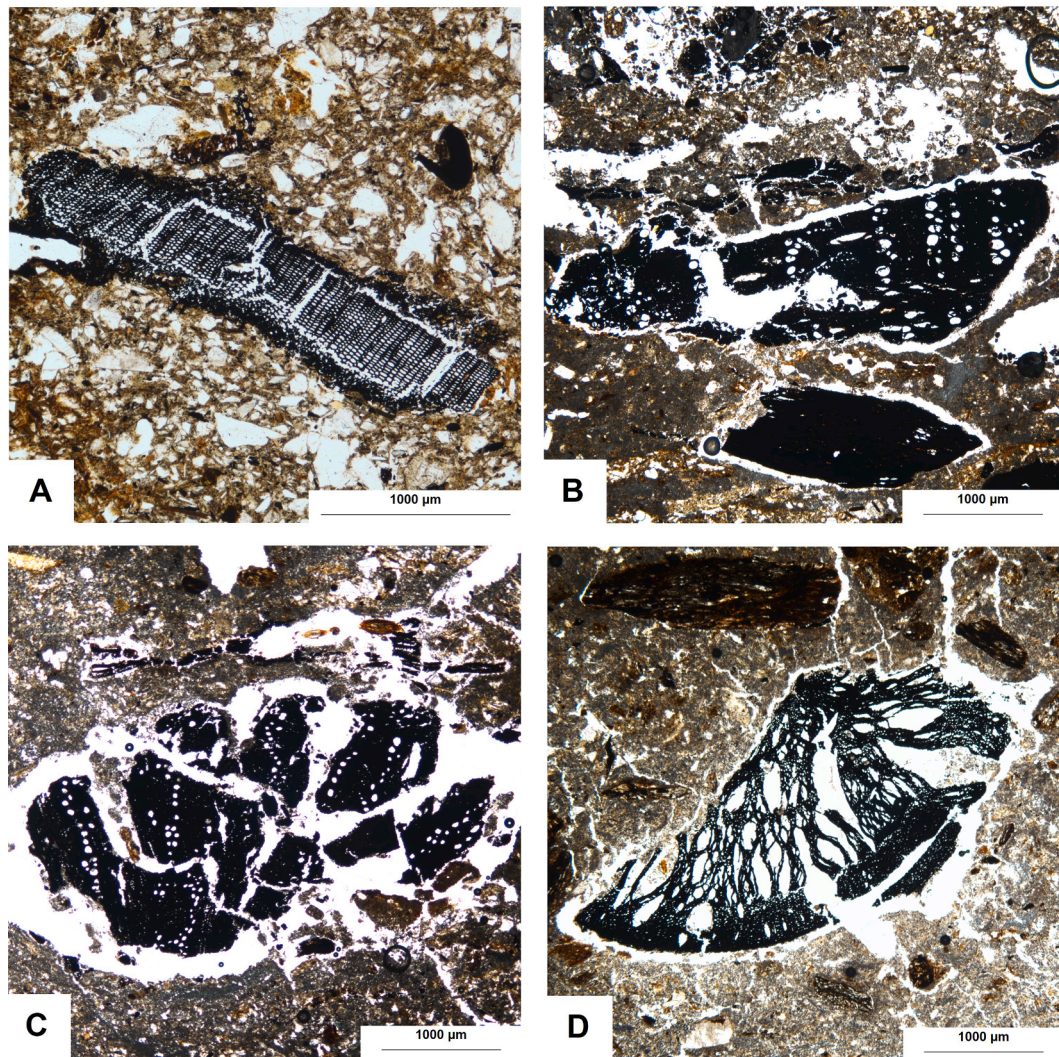


Fig. 7. Microphotographs (PPL) displaying some of the charcoal fragments identified in thin section. Cross sections of A) *Pinus* sp., B) deciduous *Quercus*, C) evergreen *Quercus*, and D) dicot.

This homogeneous molecular record points towards the presence of a strong link between the daily activities performed inside House 1 and the formation of Midden 1, supporting the hearth rake-out interpretation. In fact, the nature and components of the fire-related activities performed in House 1 do not appear to have significantly changed in the time interval covered by our samples. However, variations in the presence/absence of certain compounds could also be attributed to factors such as the degree of organic preservation. In fact, the average OEP value in this section of the deposit (3.14) (supplementary material, S9) indicates overall poor preservation, likely due to the burning processes that affected the organic molecular record and/or insect and root bioturbation, which was documented micromorphologically. Nevertheless, the differences between the molecular records of House 1 and Midden 1, and those of Midden 2 (see section 4.1.) and its adjacent dwellings (House 2 and Ancillary Structure), reinforce the existence of a link between House 1 and its external midden deposit.

4.3. Formation processes and everyday life at Cerro de San Vicente

The microcontextual geoarchaeological approach applied to the midden deposits of CSV has allowed us to identify two main formation processes: 1) the deposition of ashes and charred residues in Midden 1, and 2) the accumulation of disintegrated and intact earth-based construction materials, documented in both Midden 1 and Midden 2. As

discussed above, these middens are entirely anthropogenic in origin. This implies that the processes that led to their formation are closely related to the performance of specific cultural, everyday practices.

4.3.1. Midden 1: Construction and maintenance practices

The bottom of the sequence of Midden 1 (Fig. 11) consists of disintegrated earth-based construction materials, mixed with combustion refuse (e.g. wood ash, charcoal, burnt animal bone). Mineralogical and geochemical data indicates abundance of siliceous sediments, showing a maximum value of siliciclastic minerals (quartz, clay minerals and feldspars) and related geochemical elements (SiO_2 , Al_2O_3 and Fe_2O_3) (Fig. 9, Fig. 11). Stratigraphically, this basal unit is associated with the lowest section of the walls of House 1 (see Fig. 2), which corresponds to one of the latest identified construction phases documented in this area of the village (Blanco-González et al., 2022, 2017). Therefore, it is likely that the accumulation of earth-based construction materials at the bottom of Midden 1, along with subsequent trampling and disintegration, is associated with the construction of buildings (i.e. House 1) from this upper-intermediate phase in the history of the village. This layer could have formed as a result of the manufacturing and/or intensive use of earth-based construction materials within the village. Micromorphological observations indicate this would include both the manufacture/use of mudbrick (MFT 5) and earth-based construction floors (MFT 2), as part of recurrent and dynamic cycles of construction, refurbishment and

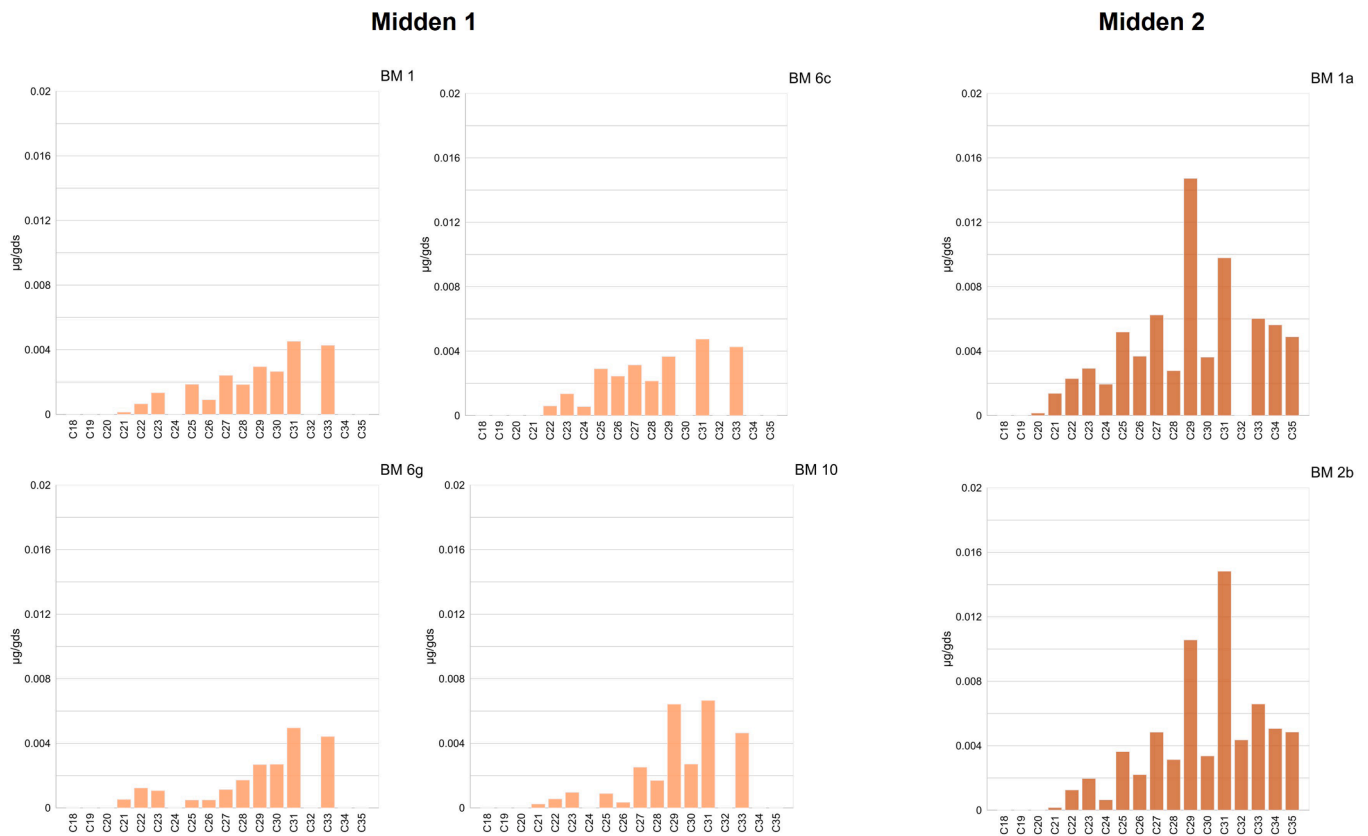


Fig. 8. Representative sedimentary *n*-alkane histograms of Midden 1 and Midden 2. In both sequences, *n*-C₂₉, *n*-C₃₁, and *n*-C₃₃ are the predominant *n*-alkanes. Note that the *n*-alkane concentrations are higher in the sequence of Midden 2.

maintenance of the buildings. In fact, it has already been proposed that communal spaces in villages may have been used for communal economic activities, such as mudbrick manufacturing (Love, 2012; Shillito and Matthews, 2013).

There is a clear shift in the stratigraphy and the mineralogical and geochemical composition of Midden 1 on the middle section (Fig. 11). This unit includes calcite and calcium rich ashy sediments with profuse archaeological remains. According to magnetic susceptibility and magnetic properties data, these layers reached burning temperatures of 700 °C (see supplementary material, S14). These multiple, micro-stratified ash-rich layers have been interpreted as the result of repeated hearth-rake out events (see section 4.2). This is further reinforced by the presence of abundant unburnt, consumed animal bone, as well as charcoal and pottery fragments, documented during the excavation of these layers (Blanco-González et al., 2022). These microfacies contain microscopic, burnt earth-based construction material fragments, exhibiting features similar to those of intact earth-based construction materials documented inside House 1 (MFT 2). Additionally, the molecular records from both the exterior of House 1 (Midden 1) and the floor sequences inside show similar characteristics, suggesting a connection between the external deposits and the activities performed inside the dwelling. Consequently, these hearth rake-out events can be associated with the cleaning and maintenance of the central clay hearth of House 1. Hearth rake-out and cleaning practices have been previously interpreted as the result of routine maintenance (Goldberg et al., 2009; Mallol et al., 2017; Nicosia et al., 2022; Oikonomou, 2023; Shillito et al., 2011b; Villagran et al., 2017) and intensive use of space (Schiffer, 1983, 1976, 1972), and thus the formation of these deposits would be associated with a period of active occupation of House 1 and nearby buildings. The disposal of ashes in communal areas has been documented in other archaeological contexts (Hayden and Cannon, 1983; Matthews, 2010; Shahack-Gross et al., 2023; Shillito and Mackay, 2020; Shillito

and Matthews, 2013). In fact, the use of fire and ashes has been previously interpreted as a useful practice for preventing the spread of bacteria and parasites (Hakbijl, 2002; Milek, 2012; Nicosia et al., 2022). It is possible that Midden 1 played a similar role in CSV, especially considering the abundance of unburnt faunal remains documented in this area during excavation, and which have been interpreted as culinary disposal (Blanco-González et al., 2022). Deposits with a potentially similar genesis and function have been documented in excavations at CSV adjacent to other structures in the village, such as those near Building 3 (Blanco-González et al., 2023a). Some of these spaces have been proposed as semi-covered areas, possibly sheltered by roofs and/or other structures (Blanco-González et al., 2022, 2023a).

The upper section of Midden 1 exhibits features similar to those found at the bottom (Fig. 11). There is an abundance of earth-based construction materials, and quartz, clay minerals and other related geochemical elements show higher concentrations. However, wood ash and charcoal fragments are more abundant in this upper section, which is quite compact. Inside House 1, a firing event is recorded atop the earthen floor sequence. It has been interpreted that this firing event was followed by the dismantling of part of the house walls, which were made of mudbrick, and that this material was then used to fill the interior of the dwelling (Blanco-González et al., 2022). Furthermore, the identification of *Pinus* sp. pinea-pinaster in previous charred wood analysis was interpreted as the remains of building material affected by the fire (Blanco-González et al., 2022). According to this interpretation, the upper section of Midden 1 would be stratigraphically associated with this destruction and dismantling phase. This would have led to the accumulation of combustion residues from the firing of the house and earth-based construction materials and their subsequent disintegration, which were then trampled and incorporated into the ashy deposit. In fact, magnetic properties analysis showed that these layers probably reached temperatures between 400 °C and 700 °C, further supporting

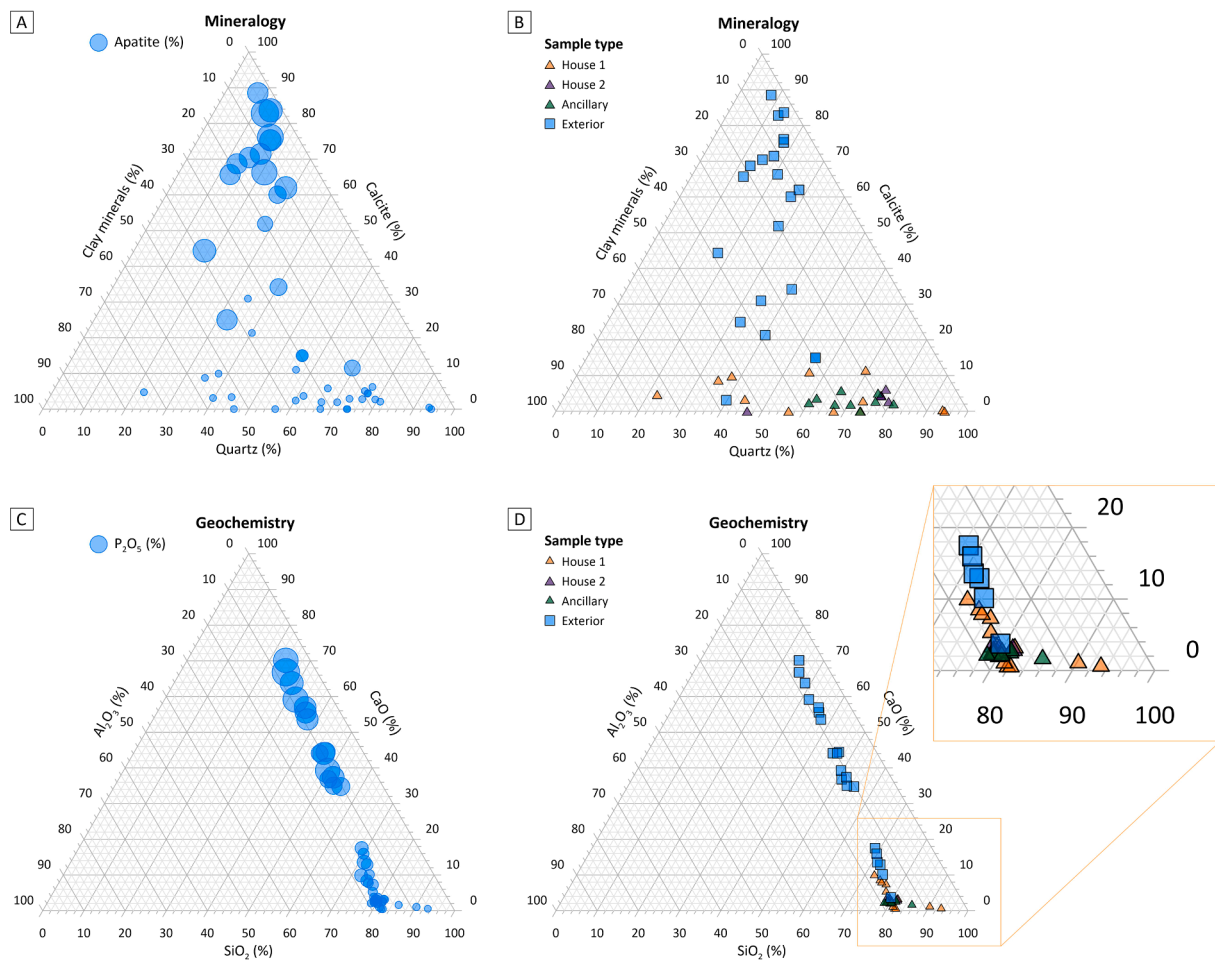


Fig. 9. Mineralogical (XRD) (A and B) and geochemical (XRF) (C and D) data of Midden 1 and Midden 2 sediment samples (blue circles and squares), compared to construction material samples (mudbrick, earth-based clay floors) from House 1, House 2 and Ancillary Structure (data taken from Tomé et al., 2024). Note the variable amount of Calcite and CaO in the midden samples.

this interpretation. Nevertheless, the hypothesis on the firing and destruction of House 1 needs to be further tested and addressed in future geoarchaeological investigations.

4.3.2. Midden 2: Plant waste and construction materials

Midden 2 primarily consists of recurrent accumulations of earth-based construction materials and frequent waste disposal, particularly wood ash, charcoal, and animal bone. Notably, the spatial proximity of Midden 2 to House 2 the Ancillary Structure and House 4 (Fig. 2) suggests a close relationship between these structures and the midden deposit. Furthermore, lipid data reveals similarities between the molecular composition of the midden deposit and that found within the dwellings (Tomé et al., 2024), including the presence of both angiosperm and conifer-specific biomarkers, mid and long-chain fatty acids and cholesterol. In addition, the presence of wood ash and charcoal fragments from various taxa, such as *Pinus* and *Quercus* sp., likely reflects maintenance activities conducted within the dwellings, specifically House 2 and/or House 4, both of which feature central clay hearths. However, the identification of microscopic fresh organic tissue and well-preserved phytoliths, predominantly monocots, in the lower-middle section of the deposit suggests a more diverse range of waste disposal practices within this sector of the village.

The phytoliths that have been identified are predominantly monocots (92 % average) and particularly ELONGATE DENTATE, which commonly derive from Poaceae inflorescence (41.8 % average) (Fig. 6, supplementary material S6). PAPILLATE was also detected, but in lower proportions. Sedimentary *n*-alkane data also points towards this direction,

which yielded *n*-C₃₁ and *n*-C₃₃ as predominant *n*-alkanes, usually associated with herbaceous input (Cranwell, 1973; Freeman and Pancost, 2014). Therefore, it is likely that discarded herbaceous taxa were recurrently deposited in Midden 2. In the context of Early Iron Age in the Central Iberian Plateau (900–400 BCE), it is widely accepted that these past communities relied on agriculture as a central economic practice (Álvarez-Sanchís, 2000), involving the regular use and exploitation of crops such as wheat, barley and oats (Delibes de Castro et al., 1995; Delibes de Castro and Romero Carnicero, 2011; Ruiz Zapatero and Álvarez-Sanchís, 2015). In fact, the middens at the central courtyard of the targeted sector have yielded abundant storage and cooking wares –including portable stoves and ceramic trays for bread–, as well as quern stones and consumed bones (Blanco-González et al., 2022, 2023a). This evidence, together with our phytolith and biomolecular data, supports that cereal and other food grinding and cooking were habitual domestic activities at CSV. Therefore, considering the above, the plant waste documented in Midden 2 could be associated with the disposal of herbaceous plant waste and/or cereal remains. However, the absence of diagnostic phytolith morphotypes for cereal crops, such as ELONGATE DENDRITIC (Albert et al., 2008) hampers a more precise taxonomic identification. Additional research on the site's microbotanical record, particularly through the analysis of bulk sediment samples from the Midden 2 sequence, is needed to confirm this hypothesis and achieve a more robust taxonomic resolution in the phytolith record (Zurro et al., 2016).

The Ancillary Structure has been previously interpreted as a storage facility; the foundation of above-ground silos for plant-based goods

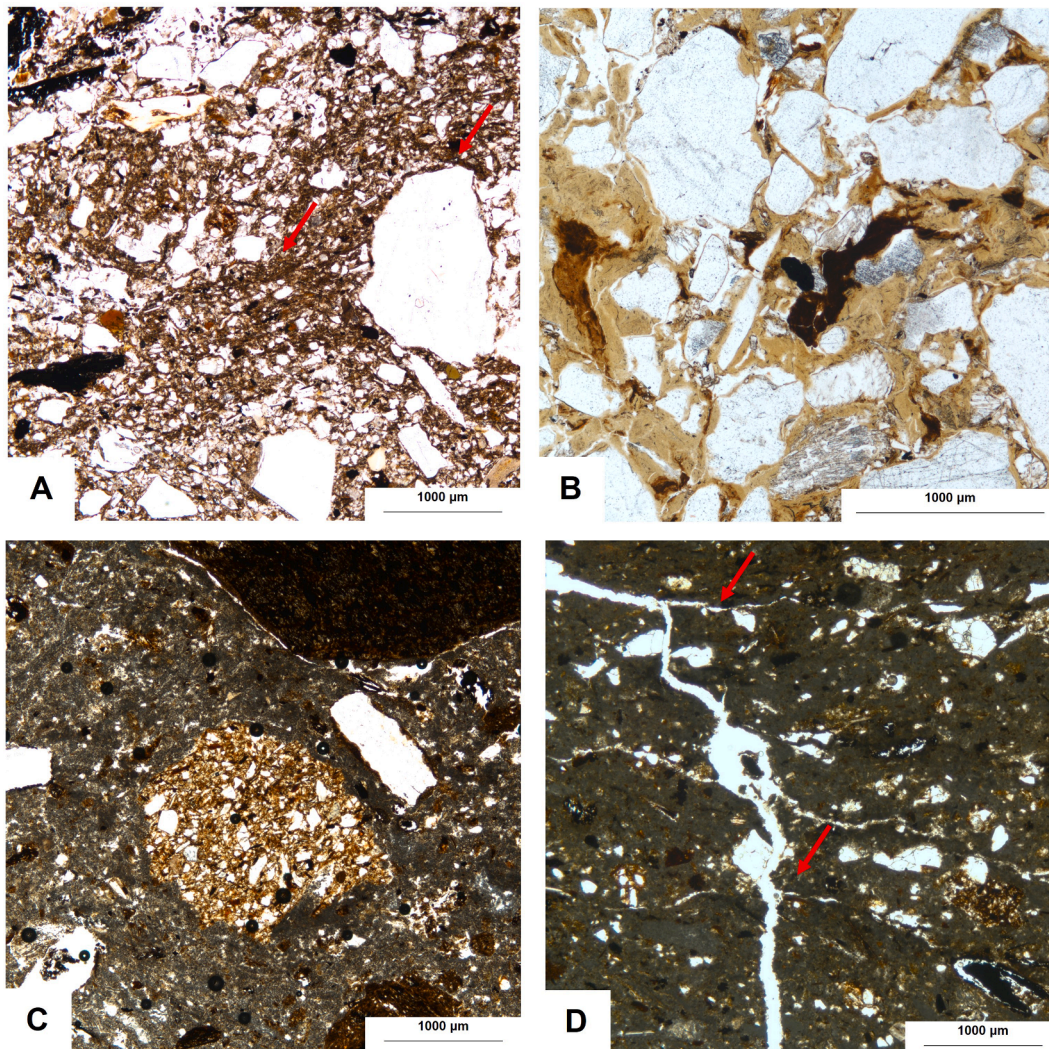


Fig. 10. Microphotographs (PPL) displaying recurrent micromorphological features and components. **A)** Midden 2. Disintegrated earth-based construction material in a sandy-clayey matrix with anthropogenic components, including charred plant matter (top). Note the presence of subhorizontally bedded clay microlaminations (arrow). These features have been previously identified in earth-based constructed floors at Cerro de San Vicente (MFT 2; Tomé et al., 2024). **B)** Midden 2. Earth-based floor preparation material fragment (MFT 1b; Tomé et al., 2024), composed of iron-stained light-yellow clay and medium-to-coarse quartz sand fragments. **C)** Midden 1. Anorthic nodule of earth-based construction material, embedded in a calcitic wood ash-rich matrix. **D)** Midden 1. Massive, compact and diffusely bedded calcitic matrix with vertical and subhorizontal planes (arrows).

(Blanco-González et al., 2022, 2017). If that was indeed its functionality, a connection between the waste disposed in Midden 2 and the products that would have been stored inside the dwelling can be proposed. In fact, micromorphological analysis revealed a stratigraphic link between Midden 2 and the earth-based floors of the Ancillary Structure and House 2. At the top of the midden sequence, fragments of a specific earth-based preparation floor resembling those found within the dwellings were documented (MFT 1b) (Fig. 10B). The use of this earth-based construction material is stratigraphically constrained to specific layers within the dwellings of this area of the village, suggesting synchronous construction processes. The finding of these earth-based preparation floor fragments in Midden 2 supports the existence of a stratigraphic, spatial, and temporal link between the deposits inside and outside the dwellings in this area of CSV. However, further geoarchaeological microcontextual data from other dwellings and midden deposits within the village is required to confirm this preliminary interpretation.

5. Conclusions

The microcontextual geoarchaeological study of midden deposits at CSV has allowed us to identify and characterize the formation processes of these complex, microstratified sequences deposited in the unroofed shared areas of the village. Through the combination of soil micromorphology –including phytolith and charcoal analysis on thin sections–, sedimentary lipid biomarkers, XRD, XRF and magnetic properties analyses, we have shown that the midden sequences are primarily anthropogenic, indicating a close relationship between their formation and the everyday practices performed within the village. Specifically, Midden 1 contains trampled earth-based construction materials and hearth rake-out debris, which is indirect evidence of building and maintenance activities inside House 1. In Midden 2, there is also evidence of discard and trampling of earth-based construction materials and hearth rake-out debris, along with a notable *input* of heterogeneous plant remains possibly linked to spatially-related communal storage and disposal practices. Based on micromorphological, mineralogical and geochemical features and their sedimentary molecular record, we have established a stratigraphic link between the deposits inside the

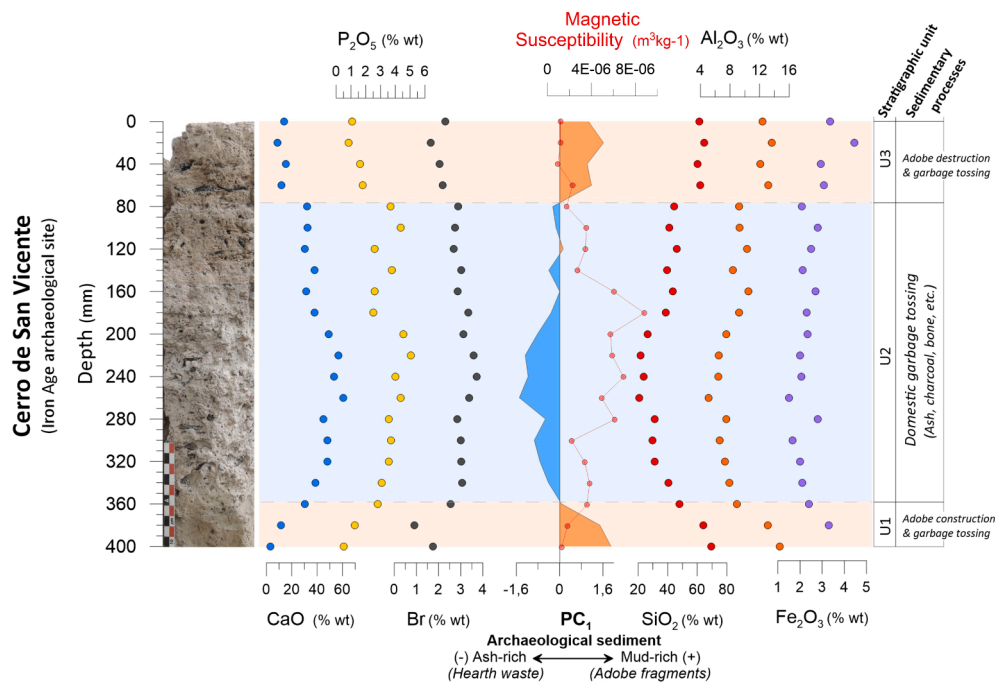


Fig. 11. Main geochemical elements and their variation along the sedimentary sequence of Midden 1. PC₁ shows the prevalence of ash-related elements in the middle part of the sequence, which gradually becomes enriched in elements related to the greater presence of silicate minerals (earth-based construction materials) towards the base and roof of the sequence. A magnetic susceptibility (MS) profile expressed by mass is also shown. Earth-based construction material-rich layers correlate with lower MS values, while ash-rich deposits exhibit higher MS values.

dwelling and the midden deposits outside. This connection has enabled us to relate these deposits to one of the village's usage cycles, in which recurrent collaborative maintenance practices—fire use, sweeping, dumping, building and/or refurbishment—resulted in the eventual accumulation of discarded domestic refuse. These findings provide valuable insights into the spatial and temporal dynamics of household activities, refuse disposal and space use in CSV, highlighting the significance of microcontextual geoarchaeological methods in assessing past human behaviors and settlement organization. However, further research is needed to expand this dataset to other areas of the site to confirm these interpretations and enhance our understanding of the broader village context. This would provide a more comprehensive, detailed understanding of daily life practices during the Early Iron Age in the Central Iberian Plateau.

Funding

This research was funded by the Spanish Ministry of Science and Innovation (Project PID2019-104349GA-I00, AEI/<https://doi.org/10.13039/501100011033>) and a predoctoral contract awarded to LT (TESIS2021010119), co-funded by the Agencia Canaria de Investigación, Innovación y Sociedad de la Información de la Consejería de Universidades, Ciencia e Innovación y Cultura, and by the European Social Fund Plus (ESF+) Integrated Operational Program of the Canary Islands 2021–2027, Axis 3 Priority Theme 74 (85 %). AC acknowledges the project PID2019105796GB-I00 of the Agencia Estatal de Investigación and project BU037P23 of Junta de Castilla y León and the European Regional Development Fund.

CRediT authorship contribution statement

Laura Tomé: Writing – original draft, Visualization, Resources, Investigation, Formal analysis, Conceptualization. **Eneko Iriarte:** Writing – review & editing, Visualization, Validation, Investigation, Formal analysis, Conceptualization. **Antonio Blanco-González:** Writing – review & editing, Visualization, Supervision, Resources,

Project administration, Funding acquisition, Conceptualization. **Enrique Fernández-Palacios:** Writing – review & editing, Visualization, Investigation, Formal analysis. **María Martín-Seijo:** Writing – review & editing, Visualization, Investigation, Formal analysis. **Ángel Carrancho:** Writing – review & editing, Visualization, Investigation, Formal analysis. **Antonio V. Herrera-Herrera:** Writing – review & editing, Validation, Data curation. **Carolina Mallo:** Writing – review & editing, Visualization, Validation, Supervision, Resources, Investigation, Formal analysis, Conceptualization.

Declaration of competing interest

The authors declare that they have no known competing financial interests or personal relationships that could have appeared to influence the work reported in this paper.

Data availability

No data was used for the research described in the article.

Acknowledgements

This research paper is a component of LT's PhD thesis, and all authors agree. The authors would like to thank Cristina Alario, Carlos Macarro and Juan Jesús Padilla for field supervision, as well as the Cerro de San Vicente excavation team for their field work. We thank Carlos Duarte Simões for supervising LT's international stay at ICAREHB (International Center for Archaeology and the Evolution of Human Behaviour, Universidade do Algarve), where part of the analyses for this article were conducted. We are thankful to Santiago Sossa for helping in the design and creation of the artwork. We thank Javier Davara for providing insightful comments on the lipid biomarker data, as well as Mónica Alonso-Eguíluz, Luc Vrydaghs and Álvaro Castilla for their suggestions regarding the phytolith analysis. We are thankful to the CENIEH and Wagner Petrographic personnel for thin section manufacture, and to the I+D+i Scientific-Technological Center (Universidad de

Burgos) personnel for performing mineralogical and geochemical analyses (XRD and XRF). Finally, we thank the anonymous reviewers who contributed to improving this research paper.

Contributions

All authors have made substantial contributions to this study. **Laura Tomé:** Conceptualization, Formal analysis, Investigation, Writing - Original Draft, Visualization; **Eneko Iriarte:** Conceptualization, Validation, Formal analysis, Investigation, Resources, Writing - Review & Editing, Visualization; **Antonio Blanco-González:** Conceptualization, Resources, Writing - Review & Editing, Visualization, Supervision, Project administration, Funding acquisition; **Enrique Fernández-Palacios:** Formal analysis, Investigation, Writing - Review & Editing, Visualization; **María Martín-Seijo:** Formal analysis, Investigation, Writing - Review & Editing, Visualization; **Ángel Carrancho:** Formal analysis, Investigation, Writing - Review & Editing, Visualization; **Antonio V. Herrera-Herrera:** Validation, Data Curation, Writing - Review & Editing; **Carolina Mallol:** Conceptualization, Validation, Formal Analysis, Investigation, Resources, Writing - Review & Editing, Visualization, Supervision.

Competing Interests.

The authors have no competing interests to declare that are relevant to the content of this article.

Appendix A. Supplementary material

Supplementary data to this article can be found online at <https://doi.org/10.1016/j.jasrep.2024.104773>.

References

- Akkemik, Ü., Yaman, B., 2012. Wood anatomy of Eastern Mediterranean species. Kessel Publishing House, Remagen.
- Albert, R.M., Shahack-Gross, R., Cabanes, D., Gilboa, A., Lev-Yadun, S., Portillo, M., Sharon, I., Boaretto, E., Weiner, S., 2008. Phytolith-rich layers from the Late Bronze and Iron Ages at Tel Dor (Israel): mode of formation and archaeological significance. *J. Archaeol. Sci.* 35, 57–75. <https://doi.org/10.1016/j.jas.2007.02.015>.
- Aldeias, V., Bicho, N., 2016. Embedded behavior: Human activities and the construction of the Mesolithic Shellmound of Cabeço da Amoreira, Muge, Portugal. *Geoarchaeology* 31, 530–549. <https://doi.org/10.1002/gea.21573>.
- Aldeias, V., Goldberg, P., Sandgathe, D., Berna, F., Dibble, H.L., McPherron, S.P., Turq, A., Rezek, Z., 2012. Evidence for Neandertal use of fire at Roc de Marsal (France). *J. Archaeol. Sci.* 39, 2414–2423. <https://doi.org/10.1016/j.jas.2012.01.039>.
- Aldeias, V., Dibble, H.L., Sandgathe, D., Goldberg, P., McPherron, S.J.P., 2016. How heat alters underlying deposits and implications for archaeological fire features: A controlled experiment. *J. Archaeol. Sci.* 67, 64–79. <https://doi.org/10.1016/j.jas.2016.01.016>.
- Álvarez, M., Briz Godino, I., Balbo, A., Madella, M., 2011. Shell middens as archives of past environments, human dispersal and specialized resource management. *Quat. Int.* 239, 1–7. <https://doi.org/10.1016/j.quaint.2010.10.025>.
- Álvarez-Sanchís, J.R., 2000. The Iron Age in Western Spain (800 BC-AD 50): An Overview. *Oxf. J. Archaeol.* 19, 65–89. <https://doi.org/10.1111/1468-0092.00100>.
- Beck, M.E., Hill, M.E., 2004. Rubbish, Relatives, and Residence: The Family Use of Middens. *J. Archaeol. Method Theory* 11, 297–333. <https://doi.org/10.1023/B:JARM.0000047316.02424.7c>.
- Blanco-González, A., Alario García, C., Macarro Alcalde, C., 2017. The Earliest villages in Iron Age Iberia (800–400 BC): a view from Cerro de San Vicente (Salamanca, Spain). *Documenta Praehistorica* 44, 386.
- Blanco-González, A., Padilla Fernández, J.J., Alario García, C., Macarro Alcalde, C., Alarcón García, E., Martín Seijo, M., Chapon, L., Iriarte, E., Pazos García, R., Sanjurjo Sánchez, J., Dorado Alejos, A., Tomé, L., Mallol Duque, C., García Redondo, N., Carrancho, Á., Calvo Rathert, M., 2022. Un singular ambiente doméstico del Hierro I en el interior de la península ibérica: la casa 1 del Cerro de San Vicente (Salamanca, España). *Trabprehist* 79, 346–361. <https://doi.org/10.3989/tp.2022.12303>.
- Blanco-González, A., Padilla Fernández, J.J., Alario García, C., Macarro Alcalde, C., Dorado Alejos, A., Pazos García, R., Cerezo Fernández, R., Chapon, L., Sánchez Polo, A., 2023a. Un santuario doméstico del siglo VII a. C. de culto a Hathor-Astarté en el Cerro de San Vicente (Salamanca, España). *Trabprehist* 80, e06–e. <https://doi.org/10.3989/tp.2023.12321>.
- Blanco-González, A., Padilla-Fernández, J.J., Dorado-Alejos, A., 2023b. Mobile craftspeople and orientalisering transculturation in seventh-century BC Iberia. *Antiquity* 1–19. <https://doi.org/10.15184/aqy.2023.96>.
- Brittingham, A., Hren, M.T., Hartman, G., 2017. Microbial alteration of the hydrogen and carbon isotopic composition of n-alkanes in sediments. *Org. Geochem.* 107, 1–8. <https://doi.org/10.1016/j.orggeochem.2017.01.010>.
- Brönnimann, D., Röder, B., Spichtig, N., Rissanen, H., Lassau, G., Rentzel, P., 2020. The Hidden Midden: Geoarchaeological investigation of sedimentation processes, waste disposal practices, and resource management at the La Tène settlement of Basel-Gasfabrik (Switzerland). *Geoarchaeology* 35, 522–544. <https://doi.org/10.1002/gea.21787>.
- Butler, D.H., Dunseth, Z.C., Tepper, Y., Erickson-Gini, T., Bar-Oz, G., Shahack-Gross, R., 2020. Byzantine-Early Islamic resource management detected through micro-geoarchaeological investigations of trash mounds (Negev, Israel). *PLoS One* 15, e0239227.
- Courty, M.-A., 2001. Microfacies Analysis Assisting Archaeological Stratigraphy. In: Goldberg, P., Holliday, V.T., Reid Ferring, C. (Eds.), *Earth Sciences and Archaeology*. Springer, US, pp. 205–239. https://doi.org/10.1007/978-1-4615-1183-0_8.
- Cranwell, P.A., 1973. Chain-length distribution of n-alkanes from lake sediments in relation to post-glacial environmental change. *Freshw. Biol.* 3, 259–265.
- Davara, J., Jambrina-Enríquez, M., Rodríguez de Vera, C., Herrera-Herrera, A.V., Mallol, C., 2023. Pyrotechnology and lipid biomarker variability in pine tar production. *Archaeol. Anthropol. Sci.* 15, 133. <https://doi.org/10.1007/s12520-023-01829-x>.
- Debels, P., Drieu, L., Chiquet, P., Studer, J., Malergue, A., Martignac, L., Champion, L., Garnier, A., Fichet, V., Sall, M., Regert, M., Mayor, A., 2024. Investigating grandmothers' cooking: A multidisciplinary approach to foodways on an archaeological dump in Lower Casamance. *Senegal. Plos One* 19, e0295794.
- Delibes de Castro, G., Romero Carnicero, F., Ramírez Ramírez, M.L., 1995. El poblado "céltico" de El Soto de Medinilla (Valladolid), in: Delibes de Castro, G., Romero Carnicero, F., Morales, A. (Eds.), *Arqueología y Medio Ambiente. El Primer Milenio A. C. En El Duero Medio*. Junta de Castilla y León, Valladolid, pp. 149–177.
- Delibes de Castro, G., Romero Carnicero, F., 2011. La plena colonización agraria del Valle Medio del Duero. *Complutum* 22, 49–94.
- Diefendorf, A.F., Freeman, K.H., Wing, S.L., Graham, H.V., 2011. Production of n-alkyl lipids in living plants and implications for the geologic past. *Geochim. Cosmochim. Acta* 75, 7472–7485. <https://doi.org/10.1016/j.gca.2011.09.028>.
- Duarte, C., Iriarte, E., Diniz, M., Arias, P., 2019. The microstratigraphic record of human activities and formation processes at the Mesolithic shell midden of Poços de São Bento (Sado Valley, Portugal). *Archaeol. Anthropol. Sci.* 11, 483–509. <https://doi.org/10.1007/s12520-017-0519-0>.
- Dunlop, D.J., Ödzemir, Ö., 1997. *Rock Magnetism: Fundamentals and Frontiers*. Cambridge University Press, New York, p. 573.
- Fernández-Palacios, E., Jambrina-Enríquez, M., Mentzer, S.M., Rodríguez de Vera, C., Dínkal, A., Égüez, N., Herrera-Herrera, A.V., Navarro Mederos, J.F., Marrero Salas, E., Miller, C.E., Mallol, C., 2023. Reconstructing formation processes at the Canary Islands indigenous site of Belmaco Cave (La Palma, Spain) through a multiproxy geoarchaeological approach. *Geoarchaeology*. doi: 10.1002/gea.21972.
- Freeman, K.H., Pancost, R.D., 2014. Biomarkers for Terrestrial Plants and Climate, in: *Treatise on Geochemistry*. Elsevier, pp. 395–416. doi: 10.1016/b978-0-08-095975-7.01028-7.
- Friesem, D., Boaretto, E., Eliyahu-Behar, A., Shahack-Gross, R., 2011. Degradation of mud brick houses in an arid environment: a geoarchaeological model. *J. Archaeol. Sci.* 38, 1135–1147. <https://doi.org/10.1016/j.jas.2010.12.011>.
- Friesem, D.E., Karkanas, P., Tsartsidou, G., Shahack-Gross, R., 2014. Sedimentary processes involved in mud brick degradation in temperate environments: a micromorphological approach in an ethnoarchaeological context in northern Greece. *J. Archaeol. Sci.* 41, 556–567. <https://doi.org/10.1016/j.jas.2013.09.017>.
- García-Redondo, N., Calvo-Rathert, M., Carrancho, Á., Goguitchaichvili, A., Iriarte, E., Blanco-González, A., Dekkers, M.J., Morales-Contreras, J., Alario-García, C., Macarro-Alcalde, C., 2021. Further evidence of high intensity during the Levantine iron age anomaly in southwestern Europe: Full vector archeomagnetic dating of an early iron age dwelling from western Spain. *J. Geophys. Res. [solid Earth]* 126. <https://doi.org/10.1029/2021jb022614>.
- Goldberg, P., Schiegl, S., Meline, K., Dayton, C., Conard, N.J., 2003. Micromorphology and site formation at Hohle Fels cave, Schwabian Jura, Germany. *E&G Quaternary Science Journal* 53, 1–25. <https://doi.org/10.3285/eg.53.1.01>.
- Goldberg, P., Miller, C.E., Schiegl, S., Ligouis, B., Berna, F., Conard, N.J., Wadley, L., 2009. Bedding, hearths, and site maintenance in the Middle Stone Age of Sibudu Cave, KwaZulu-Natal, South Africa. *Archaeol. Anthropol. Sci.* 1, 95–122. <https://doi.org/10.1007/s12520-009-0008-1>.
- Goodman-Elgar, M., 2008. The devolution of mudbrick: ethnoarchaeology of abandoned earthen dwellings in the Bolivian Andes. *J. Archaeol. Sci.* 35, 3057–3071. <https://doi.org/10.1016/j.jas.2008.05.015>.
- Gur-Arieh, S., Shahack-Gross, R., Maier, A.M., Lehmann, G., Hitchcock, L.A., Boaretto, E., 2014. The taphonomy and preservation of wood and dung ashes found in archaeological cooking installations: case studies from Iron Age Israel. *J. Archaeol. Sci.* 46, 50–67. <https://doi.org/10.1016/j.jas.2014.03.011>.
- Gutiérrez-Rodríguez, M., Bernal-Casasola, D., Díaz Rodríguez, J.J., Vargas Girón, J.M., Moujoud, T., 2022. The Urban Biography of a Mauritanian City: Microstratigraphic Analysis of the Eastern Quarter of Tamuda (Morocco). *Afr. Archaeol. Rev.* <https://doi.org/10.1007/s10437-022-09506-5>.
- Gutiérrez-Zugasti, I., Andersen, S.H., Araújo, A.C., Dupont, C., Milner, N., Monge-Soares, A.M., 2011. Shell midden research in Atlantic Europe: State of the art, research problems and perspectives for the future. *Quat. Int.* 239, 70–85. <https://doi.org/10.1016/j.quaint.2011.02.031>.
- Hakbijl, T., 2002. The Traditional, Historical and Prehistoric Use of Ashes as an Insecticide, with an Experimental Study on the Insecticidal Efficacy of Washed Ash. *Environ. Archaeol.* 7, 13–22. <https://doi.org/10.1179/env.2002.7.1.13>.

- Hayden, B., Cannon, A., 1983. Where the garbage goes: Refuse disposal in the Maya Highlands. *J. Anthropol. Archaeol.* 2, 117–163. [https://doi.org/10.1016/0278-4165\(83\)90010-7](https://doi.org/10.1016/0278-4165(83)90010-7).
- Herrera-Herrera, A.V., Mohamed-Rodríguez, N., Socas-Rodríguez, B., Mallol, C., 2020. Development of a QuEChERS-based method combined with gas chromatography-mass spectrometry for the analysis of alkanes in sediments. *Microchem. J.* 155, 104774. <https://doi.org/10.1016/j.microc.2020.104774>.
- Hoefs, M.J.L., Rijpstra, W.I.C., Sinnighe Damsté, J.S., 2002. The influence of oxic degradation on the sedimentary biomarker record I: evidence from Madeira Abyssal Plain turbidites. *Geochim. Cosmochim. Acta.* [https://doi.org/10.1016/S0016-7037\(02\)00864-5](https://doi.org/10.1016/S0016-7037(02)00864-5).
- ICPT (Neumann, K., Strömberg, C.A.E., Ball, T.B., Albert, R.M., Vrydaghs, L., Scott Cummings, L.), 2019. International Code for Phytolith Nomenclature (ICPN) 2.0. *Ann. Bot.* 124 (2), 189–199. <https://doi.org/10.1093/aob/mcz064>.
- Karkanias, P., 2021. All about wood ash: Long term fire experiments reveal unknown aspects of the formation and preservation of ash with critical implications on the emergence and use of fire in the past. *J. Archaeol. Sci.* 135, 105476. <https://doi.org/10.1016/j.jas.2021.105476>.
- Leierer, L., Jambriña-Enríquez, M., Herrera-Herrera, A.V., Connolly, R., Hernández, C. M., Galván, B., Mallol, C., 2019. Insights into the timing, intensity and natural setting of Neanderthal occupation from the geoarchaeological study of combustion structures: A micromorphological and biomarker investigation of El Salt, unit Xb, Alcoy, Spain. *Plos One* 14, e0214955.
- Lisá, L., Kočár, P., Bajer, A., Kočárová, R., Syrová, Z., Syrový, J., Porubčanová, M., Lisý, P., Peska, M., Ježková, M., 2020. The floor: a voice of human lifeways—a geo-ethnographical study of historical and recent floors at Dolní Němčí Mill, Czech Republic. *Archaeol. Anthropol. Sci.* 12, 115. <https://doi.org/10.1007/s12520-020-01060-y>.
- Love, S., 2012. The geoarchaeology of mudbricks in architecture: A methodological study from Çatalhöyük, Turkey: Geoarchaeology of mudbricks in architecture. *Geoarchaeology* 27, 140–156. <https://doi.org/10.1002/geoa.21401>.
- Macarro Alcalde, C., Alario García, C., 2021. Los orígenes de Salamanca. El poblado protohistórico del Cerro de San Vicente. Centro de Estudios Salmantinos, Salamanca.
- Mackenzie, A.S., Brassell, S.C., Eglinton, G., Maxwell, J.R., 1982. Chemical fossils: the geological fate of steroids. *Science* 217, 491–504. <https://doi.org/10.1126/science.217.4559.491>.
- Mallol, C., Hernández, C.M., Cabanes, D., Machado, J., Sistiaga, A., Pérez, L., Galván, B., 2013a. Human actions performed on simple combustion structures: An experimental approach to the study of Middle Palaeolithic fire. *Quat. Int.* 315, 3–15. <https://doi.org/10.1016/j.quaint.2013.04.009>.
- Mallol, C., Hernández, C.M., Cabanes, D., Sistiaga, A., Machado, J., Rodríguez, Á., Pérez, L., Galván, B., 2013b. The black layer of Middle Palaeolithic combustion structures. Interpretation and archaeostratigraphic implications. *J. Archaeol. Sci.* 40, 2515–2537. <https://doi.org/10.1016/j.jas.2012.09.017>.
- Mallol, C., Mentzer, S.M., Miller, C.E., 2017. Combustion features. In: Nicosia, C., Stoops, G. (Eds.), *Archaeological Soil and Sediment Micromorphology*. Wiley Blackwell, Oxford, pp. 299–330.
- Marczagan, D., Miller, C.E., Conard, N.J., 2022. Burning, dumping, and site use during the Middle and Upper Palaeolithic at Hohle Fels Cave, SW Germany. *Archaeol. Anthropol. Sci.* 14, 178. <https://doi.org/10.1007/s12520-022-01647-7>.
- Marquer, L., Otto, T., 2020. Microscopic Charcoal Signal in Archaeological Contexts. In: Henry, A.G. (Ed.), *Handbook for the Analysis of Micro-Particles in Archaeological Samples*. Springer, pp. 225–254.
- Matthews, W., 2005. Micromorphological and microstratigraphic traces of uses and concepts of space. In: Hodder, I. (Ed.), *Inhabiting Catalhöyük: Reports from the 1995–1999 Seasons*. McDonald Institute for Archaeological Research and British Institute of Archaeology at Ankara, Cambridge.
- Matthews, W., 2010. Geoarchaeology and taphonomy of plant remains and microarchaeological residues in early urban environments in the Ancient Near East. *Quat. Int.* 214, 98–113. <https://doi.org/10.1016/j.quaint.2009.10.019>.
- Meignen, L., Goldberg, P., Bar-Yosef, O., 2007. The Hearths at Kebara Cave and their Role in Site Formation Processes, in: Bar-Yosef O Meignen (Ed.), Kebara Cave Mt. Carmel, Israel. The Middle and Upper Palaeolithic Archaeology, Part I, American School of Prehistoric Research Bulletin. Peabody Museum of Archaeology and Ethnology, Harvard University, Cambridge, pp. 91–122.
- Mendes Cardoso, J., Merencio, F., Villagrán, X., Wesolowski, V., Estevam, R., Fuller, B.T., DeBlasis, P., Pierre-Gilson, S., Guiserix, D., Méjean, P., Figuti, L., Farias, D., Guimaraes, G., Strauss, A., Jaouen, K., 2024. Late shellmound occupation in southern Brazil: A multi-proxy study of the Galheta IV archaeological site. *PLoS One* 19, e0300684.
- Mentzer, S.M., 2014. Microarchaeological approaches to the identification and interpretation of combustion features in prehistoric archaeological sites. *J. Archaeol. Method Theory* 21, 616–668. <https://doi.org/10.1007/s10816-012-9163-2>.
- Milek, K.B., 2012. Floor formation processes and the interpretation of site activity areas: An ethnoarchaeological study of turf buildings at Thvera, northeast Iceland. *J. Anthropol. Archaeol.* 31, 119–137. <https://doi.org/10.1016/j.jaa.2011.11.001>.
- Miller, C.E., Conard, N.J., Goldberg, P., Berna, F., 2010. Dumping, sweeping and trampling: experimental micromorphological analysis of anthropogenically modified combustion features. *Paléontologie* 2. <https://doi.org/10.4000/paleontologie.8197>.
- Needham, S., Spence, T., 1997. Refuse and the formation of middens. *Antiquity* 71, 77–90. <https://doi.org/10.1017/S0003598X00084568ICPT>.
- Nicosia, C., Polisca, F., Miller, C., Ligouis, B., Mentzer, S., Mangani, C., Gonzato, F., 2022. High-resolution sediment analysis reveals Middle Bronze Age byre-houses at the site of Oppeano (Verona province, NE Italy). *PLoS One* 17, e0272561.
- Nicosia, C., Stoops, G., 2017. *Archaeological Soil and Sediment Micromorphology*. Wiley Blackwell, Oxford.
- Oikonomou, I.A.K., 2023. Deciphering Anthro-Sedimentary Processes and Ash Micro-Histories at the Neolithic Lakeside Settlement of Dispilio, Greece: A Micro-Geoarchaeological Approach. *J. Archaeol. Sci. Rep.* 49, 103948. <https://doi.org/10.1016/j.jasrep.2023.103948>.
- Oros, D.R., Simoneit, B.R.T., 2001a. Identification and emission factors of molecular tracers in organic aerosols from biomass burning Part 1. Temperate climate conifers. *Applied Geochemistry*. doi: 10.1016/S0883-2927(01)00021-x.
- Oros, D.R., Simoneit, B.R.T., 2001b. Identification and emission factors of molecular tracers in organic aerosols from biomass burning Part 2. Deciduous Trees. *Appl. Geochem.* 16, 1545–1565. [https://doi.org/10.1016/S0883-2927\(01\)00022-1](https://doi.org/10.1016/S0883-2927(01)00022-1).
- Pawłowska, K., Shillito, L.M., 2022. An Integrated Zooarchaeological and Micromorphological Perspective on Midden Taphonomy at Late Neolithic Çatalhöyük. *Open Archaeology* 8, 436–459. <https://doi.org/10.1515/par-2020-0215>.
- Piperno, D.R., 2006. *Phytoliths: A comprehensive guide for archaeologists and paleoecologists*. Altamira Press, Lanham.
- Portillo, M., García-Suárez, A., Klimowicz, A., Barański, M.Z., Matthews, W., 2019. Animal penning and open area activity at Neolithic Çatalhöyük, Turkey. *Journal of Anthropological Archaeology* 56, 101106. <https://doi.org/10.1016/j.jaa.2019.101106>.
- Poynter, J., Eglinton, G., 1990. In: Cochran, J. R. et al. (eds.) *Proceedings of the Ocean Drilling Program, Scientific Results, Vol. 116*, pp. 155–161. College Station, TX: Ocean Drilling Program.
- Rentzel, P., Nicosia, C., Gebhardt, A., Brönnimann, D., Pümpin, C., Ismail-Meyer, K., 2017. Trampling, Poaching and the Effect of Traffic. In: Nicosia, C., Stoops, G. (Eds.), *Archaeological Soil and Sediment Micromorphology*. Wiley Blackwell, Oxford, pp. 281–297.
- Rubiales, J.M., Hernández, L., Romero, F., Sanz, C., 2011. The use of forest resources in central Iberia during the Late Iron Age. Insights from the wood charcoal analysis of Pintia, a Vaccaean oppidum. *J. Archaeol. Sci.* 38, 1–10. <https://doi.org/10.1016/j.jas.2010.07.004>.
- Ruiz Zapatero, G., Álvarez-Sanchís, J.R., 2015. ¿Centros de poder? Sociedad y poblamiento en la Meseta Norte española (ca. 800–400 a.C.). *Veguetia* 15, 211–237.
- Schiegl, S., Goldberg, P., Pfretschner, H.-U., Conard, N.J., 2003. Paleolithic burnt bone horizons from the Swabian Jura: Distinguishing between *in situ* fireplaces and dumping areas. *Geoarchaeology* 18, 541–565. <https://doi.org/10.1002/geoa.10080>.
- Schiffer, M.B., 1972. Archaeological Context and Systemic Context. *Am. Antiq.* 37, 156–165. <https://doi.org/10.2307/278203>.
- Schiffer, M.B., 1976. *Behavioral Archeology*. Academic Press, Cambridge.
- Schiffer, M.B., 1983. Toward the Identification of Formation Processes. *Am. Antiq.* 48, 675–706. <https://doi.org/10.2307/279771>.
- Schweingruber, F.H., 1990. *Anatomy of European Woods. An atlas for the identification of European trees, shrubs and dwarf shrubs*. Paul Haupt, Stuttgart.
- Shahack-Gross, R., Ogllobin Ramirez, I., Zajac, P.R., Arkin Shalev, E., Zilberman, T., Yasur, G., Matskevich, S., Martin, S.R., Gilboa, A., Sharon, I., Yasur-Landau, A., 2023. Geoarchaeology at the marine waterfront of a coastal urban center: Human activities and sea-land interface processes on the Late Bronze and early Iron Age coast of Tel Dor, Israel. *Journal of Archaeological Science: Reports* 48, 103835. <https://doi.org/10.1016/j.jasrep.2023.103835>.
- Shillito, L.-M., Bull, I.D., Matthews, W., Almond, M.J., Williams, J.M., Evershed, R.P., 2011a. Biomolecular and micromorphological analysis of suspected faecal deposits at Neolithic Çatalhöyük, Turkey. *J. Archaeol. Sci.* 38, 1869–1877. <https://doi.org/10.1016/j.jas.2011.03.031>.
- Shillito, L.-M., Matthews, W., Almond, M., 2008. Investigating midden formation processes and cultural activities at Neolithic Çatalhöyük, Turkey. *Antiquity Project Gallery* 82.
- Shillito, L.-M., Mackay, H., 2020. Middens, Waste Disposal, and Health at Çatalhöyük. *Near Eastern Archaeology* 83, 168–174. <https://doi.org/10.1086/710134>.
- Shillito, L.-M., Matthews, W., Almond, M.J., Bull, I.D., 2011b. The microstratigraphy of middens: capturing daily routine in rubbish at Neolithic Çatalhöyük, Turkey. *Antiquity* 85, 1024–1038. <https://doi.org/10.1017/S0003598X00068460>.
- Shillito, L.-M., Matthews, W., 2013. Geoarchaeological investigations of midden-formation processes in the early to late ceramic neolithic levels at Çatalhöyük, turkeyca. 8550–8370 cal BP. *Geoarchaeology* 28, 25–49. <https://doi.org/10.1002/geoa.21427>.
- Shillito, L.-M., 2015. Middens and other trash deposits, in: Karen B. Metheny, M.C.B. (Ed.), *Archaeology of Food: An Encyclopedia*. Rowman & Littlefield, pp. 316–318.
- Stahlschmidt, M., Miller, C.E., Kandel, A.W., Goldberg, P., Conard, N.J., 2017. Site formation processes and Late Natufian domestic spaces at Baaz Rockshelter, Syria: A micromorphological perspective. *J. Archaeol. Sci. Rep.* 12, 499–514. <https://doi.org/10.1016/j.jasrep.2017.03.009>.
- Starkovich, B.M., Elefanti, P., Karkanias, P., Panagopoulou, E., 2020. Site Use and Maintenance in the Middle Palaeolithic at Lakonis I (Peloponnese, Greece). *Journal of Paleolithic Archaeology* 3, 157–186. <https://doi.org/10.1007/s41982-018-0006-x>.
- Stoops, G., 2003. *Guidelines for analysis and description of soil and regolith thin sections*. Soil Science Society of America, Madison.
- Tomé, L., Jambriña-Enríquez, M., Egúez, N., Herrera-Herrera, A.V., Davara, J., Marrero Salas, E., Aray de la Rosa, M., Mallol, C., 2022. Fuel sources, natural vegetation and subsistence at a high-altitude aboriginal settlement in Tenerife, Canary Islands: Microcontextual geoarchaeological data from Roques de García Rockshelter. *Archaeol. Anthropol. Sci.* 14, 195. <https://doi.org/10.1007/s12520-022-01661-9>.
- Tomé, L., Iriarte, E., Blanco-González, A., Jambriña-Enríquez, M., Egúez, N., Herrera-Herrera, A.V., Mallol, C., 2024. Searching for traces of human activity in earthen floor sequences: high-resolution geoarchaeological analyses at an Early Iron Age

- village in Central Iberia. *J. Archaeol. Sci.* 161, 105897. <https://doi.org/10.1016/j.jas.2023.105897>.
- Villagran, X.S., 2014. A redefinition of waste: Deconstructing shell and fish mound formation among coastal groups of southern Brazil. *J. Anthropol. Archaeol.* 36, 211–227. <https://doi.org/10.1016/j.jaa.2014.10.002>.
- Villagran, X.S., Strauss, A., Miller, C., Ligouis, B., Oliveira, R., 2017. Buried in ashes: Site formation processes at Lapa do Santo rockshelter, east-central Brazil. *J. Archaeol. Sci.* 77, 10–34. <https://doi.org/10.1016/j.jas.2016.07.008>.
- Vrydaghs, L., Devos, Y., 2018. Visibility, Preservation and Colour: A Descriptive System for the Study of Opal Phytoliths in (Archaeological) Soil and Sediment Thin Sections. *Environ. Archaeol.* 25, 170–177. <https://doi.org/10.1080/14614103.2018.1501867>.
- Wiesenberg, G.L.B., Lehdorff, E., Schwark, L., 2009. Thermal degradation of rye and maize straw: Lipid pattern changes as a function of temperature. *Org. Geochem.* 40, 167–174. <https://doi.org/10.1016/j.orggeochem.2008.11.004>.
- Zurro, D., García-Granero, J.J., Lancelotti, C., Madella, M., 2016. Directions in current and future phytolith research. *J. Archaeol. Sci.* 68, 112–117. <https://doi.org/10.1016/j.jas.2015.11.014>.